THE ROLE OF IBR5-AtNRPB4 INTERACTION IN ARABIDOPSIS GROWTH AND DEVELOPMENT

by

Rohit Upendra Katti, BSc., MSc.

A thesis submitted to the Graduate Council of
Texas State University in partial fulfillment
of the requirements for the degree of
Master of Science
with Major in Biology
August 2019

Committee Members:

Nihal Dharmasiri, Chair.

Hong-Gu Kang, Co-Chair.

Sunethra Dharmasiri, Co-Chair.

FAIR USE AND AUTHOR'S PERMISSION STATEMENT

Fair Use

Duplication Permission

ACKNOWLEDGEMENTS

Before getting into the thick of things, I would like to add a few heartfelt words for the people who were a part of this project in numerous ways. A heartfelt gratitude and sincere acknowledgements to my advisor Dr. Nihal Dharmasiri, for his valuable guidance, constant and active supervision and inspiration throughout this investigation, Dr. Sunethra Dharmasiri, for her words of encouragement and indispensable advice, and Dr. Hong-Gu Kang, for rendering me with his valuable insights throughout the project. I thank my parents for believing in me and for their constant support. I also extend my gratitude to my lab mates, Nicholas Siepert, Timothy Cioffi and Idrees Ahmad, and all my friends and family for encouraging me to always do my best and to pursue my goals.

TABLE OF CONTENTS

Page

LIST OF FIGURES

Figure **Page**

ABSTRACT

Auxin is a crucial plant hormone necessary for the regulation of growth and development in plants. It has been shown that Indole Butyric acid Response 5 (IBR5), which encodes a dual specificity phosphatase, is involved in the auxin signaling pathway. However, the exact molecular mechanism by which it regulates auxin signaling is not well understood. In yeast two-hybrid screen, IBR5 interacted with NRPB4, which is known to be an integral part of RNA Polymerase II complex. Previous studies on NRPB4 have shown that it is involved in thermotolerance in yeast. In Arabidopsis, NRPB4 is seen to physically interacts with IBR5 *in-vitro* confirming yeast two-hybrid result. Further analysis shows that the catalytic domain of IBR5 is important for the interaction with AtNRPB4. The biological relevance of IBR5-AtNRPB4 interaction is not yet clear, but both proteins have been linked to heat stress responses. Characterization of Arabidopsis *nrpb4* mutants show severe growth defects in hypocotyl elongation and root growth in response to high temperature showing defective auxin responses suggesting possible functional interaction between IBR5 and NRPB4 by itself or as a complex with other auxin-related protein such as HSP90. However, effort to demonstrate IBR5-NRPB4 interaction *in vivo* was not successful. Nevertheless, *in-vitro* interaction between IBR5- NRPB4 along with common defective phenotypes of *nrpb4* and *ibr5* mutants indicate a possible interaction between these two proteins.

I. INTRODUCTION

The growth and development of the plants are highly regulated processes controlled by several plant hormones and environmental factors. Since plants are sessile in nature, they have highly adapted signaling mechanisms to sense and quickly respond to the changes in environment. Many of these signaling mechanisms are regulated by several phytohormones.

Phytohormones are chemical messengers produced in plants, and they regulate the cellular processes by interacting with specific proteins functioning as receptors. Auxin was the first plant growth hormone to be studied in plants. It controls many stages of plant growth and development, primarily regulating cell division, cell elongation and cell differentiation [1]. Indole-3-acetic acid (IAA), the primary native form of auxin, is involved in regulating plant growth and development through both genomic and non-genomic pathways. Auxin regulates the expression of many growth-related genes including primary auxin responsive gene families known as GH3, Aux/IAA, and SAUR genes [3].

The most well characterized auxin signaling events are arbitrated by Auxin Responsive Elements (AREs) in the promoters of auxin responsive genes. The Auxin Response Factors (ARFs) induces the ARE mediated transcription, which can be repressed by the binding of the Aux/IAA proteins to the ARFs [2, 3]. Auxin regulates the expression of auxin-responsive genes by promoting the degradation of Aux/IAA proteins via the Ubiquitin-Proteasome Pathway System (UPS) [4, 5].

UPS is the most commonly used mechanism for targeted protein degradation by various signaling pathways, including phytohormone signaling [5]. Ubiquitin, which

serves as an identification tag for the 26S proteasome, is covalently bound to target proteins with the help of E3 ubiquitin ligases [6]. Aux/IAA proteins are one such target proteins that are polyubiquitinated by SCF (Skp1-Cullin1-F-box protein) E3 ubiquitin ligases [6]. The F-box proteins usually have a leucine-rich domain, which serve as a protein interacting domain specific for interaction with target proteins [7]. The auxin related SCF complexes comprises of core sub-units RBX1, CUL1, ASK1 (Arabidopsis SKP1- like), and the TIR1/AFB's family (Transport Inhibitor Resistance1/ Auxin Signaling F-box) as F-box proteins [36]. Auxins enhances the affinity between the F-box proteins TIR1/AFBs and the Aux/IAA protein [4, 8].

Recent studies have shown that, *INDOLE-3 BUTYRIC ACID RESPONSE 5* (*IBR5*) gene that encodes a putative dual-specificity phosphatase is involved in plant auxin response [9, 10]. All dual specificity phosphatases (DSPs) contain a catalytic domain which is responsible in removing the phosphate group attached to a tyrosine, serine or threonine residue. DSPs are a key regulatory factor in signal transduction pathways (For e.g. MAP kinase pathway). IBR5 interacts with several proteins associated with different signal transduction pathways. Some of these proteins include mitogen-activated protein kinase 12 (MPK12) [12], R proteins [13], SCF complex protein ASK1[*Jayaweera, unpublished*] and chaperone proteins like SGT1 and HSP90 [11].

The *ibr5-1* null mutation was identified through a mutant screen for primary root growth resistance to exogenous indole-3-butyric acid (IBA), a natural precursor of indole-3-acetic acid (IAA) [16]. Through a screen of ethyl methane-sulfonate (EMS) generated Arabidopsis mutants against to picloram, a synthetic auxin, our lab identified *ibr5-4*, which is a catalytic site mutant with an amino acid substitution of Gly132 with

Glu [10].

Generally, in response to auxin Aux/IAA repressor proteins are degraded with concomitant increase of auxin inducible gene expression [17, 18, 19, 20]. Interestingly, in *ibr5* mutants (*ibr5-1, ibr5-4*), while the degradation of Aux/IAA is enhanced, the expression of auxin induced- gene expression is downregulated. [9, 10].

An interaction between IBR5 and SCF complex component, ASK1 was shown via high-throughput binary interactome mapping (a modified Yeast two-hybrid system) [13]. This interaction was also confirmed *in-vivo* by immunoprecipitating IBR5-Myc with anti-Myc antibody [Figure 1]. The IBR5-ASK1 interaction indicates the relevance between IBR5 in auxin signaling pathway as well as other signaling pathways that use SCF complexes.

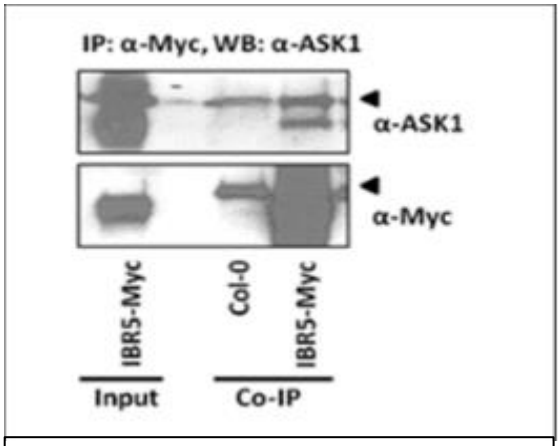

Figure 1. IBR5 interacts with ASK1 *in vivo*. Total protein collected from Col-0 and *35S::IBR5-Myc* using native extraction methods. *IBR5-Myc* was immunoprecipitated using anti-Myc agarose beads. ASK1 and *IBR5-Myc* were detected using anti-ASK1 and anti-Myc respectively. Arrows show non-specific binding of antibodies. (Jayaweera, unpublished)

To shed light on the role of IBR5 in auxin signaling, our lab identified several IBR5 interacting proteins using yeast two-hybrid screen (Kathare, unpublished). One of the IBR5 interacting proteins was identified as NUCLEAR RNA POLYMERASE B4 (NRPB4/ RPB4), an integral part of DNA dependent RNA Polymerase II (RNA Pol II). NRPB4 is the fourth subunit of the RNA Pol II enzyme [37]. Previous studies have shown that *Saccharomyces cerevisiae* RPB4 has conserved C- and N- termini regions, which are involved in the protein-protein interaction with RPB7, another subunit of RNA Pol II with which RPB4 forms a heterodimer. [14, 15].

RNA Pol II is a multi-protein complex localized to the nucleus and catalyzes transcription [21, 22]. It is a 550 kDa complex comprised of 12 subunits, NRPB1-12 [Figure 2]. NRPB4, subunit has a size of 15.9 kDa [23]. The orthologs of NRPB4 are found in *S. cerevisiae* and *Homo sapiens*. Comparison of NRPB4 amino acid sequences

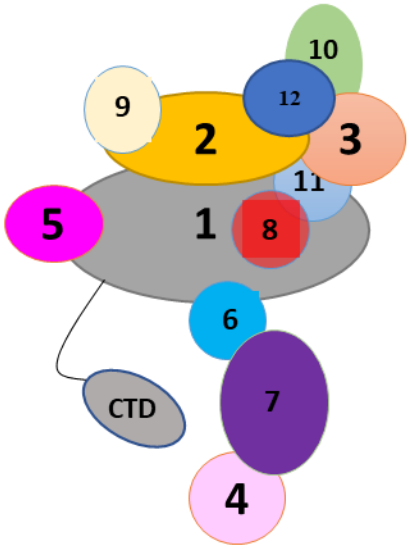

Figure 2. Structure of RNA Pol II enzyme showing 12 sub-units. Adapted from previously published data [36].

of Arabidopsis and yeast shows 67% similarity. [23, and Figure 3].

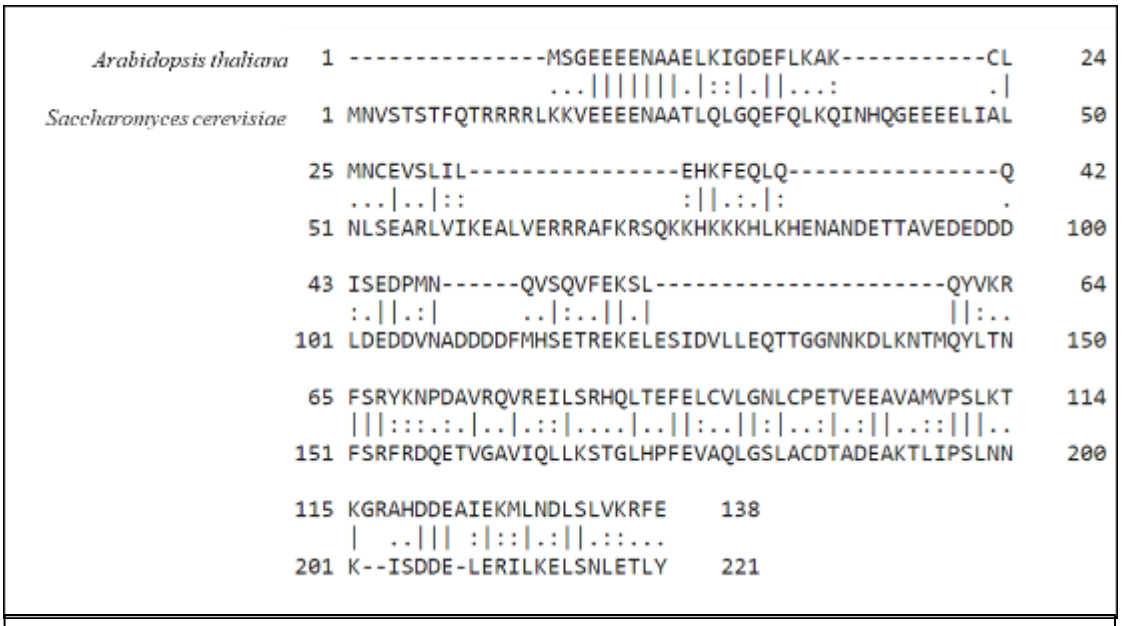

Figure 3. Comparison of amino acid sequence of NRPB4 of Arabidopsis and Yeast. The straight line (|) and dots (.) indicate identity and similarity respectively. EMBOSS Needle alignment tool was used to align the protein sequences.

Previous studies have shown that loss of RPB4 function in Yeast results in general growth defects, while the effect is more apparent at high temperature suggesting that RPB4 is necessary for thermotolerance. Interestingly, the growth rate and the rate of mRNA synthesis goes down, especially at high temperature, in *Δrpb4* mutants when compared to wild type [24, and Figure 4].

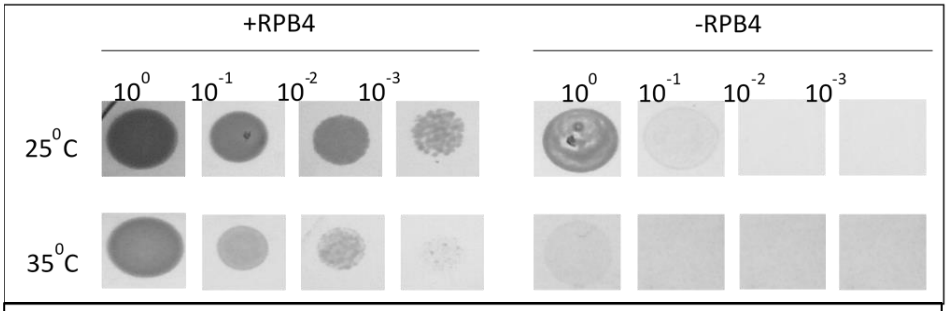

Figure 4. Wild-type RPB4 (+RPB4) and *Δrpb4* (-RPB4) show growth defects at moderate temperature and effect on the defective growth is enhanced at high-temperature. The cells were grown on rich medium (YPD).

RNA Pol II enzyme catalyzes eukaryotic mRNA transcription. in yeast, it has been shown that RPB4 is mainly involved in nuclear mRNA synthesis. Deletion of RPB4 causes a significant decrease in mRNA synthesis, which down-regulates mRNA degradation, resulting in adjustment of levels in overall mRNA synthesis and degradation rates to maintain similar mRNA concentration in the cell. This phenomenon is known as mRNA level buffering [32]. RPB4 has also been suggested to protect RNA Pol II enzyme from inactivating at high temperatures [33].

Considering NRPB4 in yeast is involved in heat stress response and shares sequence similarity with AtNRPB4, it would be compelling to see if it plays a role in plants in a similar way. Interestingly, IBR5 has also shown to be involved in heat stress responses [Cioffi, unpublished]. Since the yeast two-hybrid (Y2H) screen result show interaction between IBR5 and NRPB4, it would be interesting to assess if the interaction is true and evaluate the possible role of IBR5-AtNRPB4 interaction in plant development. Because the RNA Pol II sub-unit- NRPB4 was identified as an IBR5 interacting partner in Y2H screen, and *nrpb4* mutants showing resistance to auxins, we hypothesized that IBR5 may interact with NRPB4 *in vivo* and this interaction is involved in regulating the auxin signaling. Additionally, it is hypothesized that *nrpb4* mutation is the cause for defective *nrpb4* phenotype.

II. MATERIALS AND METHODS

Plant materials

The *Arabidopsis thaliana* ecotype *Columbia* (Col-0) was used in all experiments. *nrpb4* seeds (SALK_122761) were obtained from Arabidopsis Biological Resource Center (ABRC). Transgenic line *35S::IBR5-Myc* used in the study has been described previously (Jayaweera et.al. 2014). *ibr5*-1 seeds were courteously provided by Dr. Bonnie Bartel, Rice University.

Seed sterilization and germination

The Arabidopsis seeds were surface-sterilized using 40% bleach + 0.04% Triton X- 100 solution. The seeds were then washed four times for 10 minutes each using sterile distilled water and vernalized at 4^0C for 24 hours. The seeds were then plated on *Arabidopsis thaliana* medium having 1% Sucrose (ATS) with 0.8% Agar. The plates were incubated either vertically or horizontally depending on the experiment in a growth chamber at 22^0C with continuous light. When necessary, seedlings were grown in pots. Seedlings were transferred on to soil (Pro-Mix BX), vernalized for about 48 hours at 4^0C, and then were grown under continuous light at 22^0C.

Isolation of Genomic DNA

To isolate the genomic DNA, a single green leaf tissue (approximately 50 mg) was homogenized in 300µL 2X CTAB buffer containing 2% (w/v) cetyl trimethylammonium bromide (CTAB); 1.4M NaCl; 100mM Tris-Cl (pH-8); and 20mM EDTA. The samples were then heated at 65^0C for about 30 minutes, 300µL Chloroform was added to the homogenate, and vortexed for 10-15 seconds. It was then centrifuged at 10000 g for 5 minutes and approximately 200µL of the supernatant was transferred to a

new tube with 3 volumes of ice-cold 100% Ethanol. The tubes were then kept at -20^{0}C for at least 45 minutes and centrifuged at 10000 g for 20 minutes at 4^{0}C. The supernatant was discarded, and the pellet was washed with 300µL ice-cold 70% Ethanol by centrifuging at 10000 g for 5 minutes at 4^{0}C. The pellet was air dried and resuspended in 60µL of 10mM Tris-Cl (pH-8). The Genomic DNA samples were stored at -20^{0}C until further use.

RNA isolation and cDNA synthesis

1.1.For RNA isolation, four days-old *Arabidopsis* seedlings were flash frozen in liquid nitrogen and ground. The powder was transferred to a 1.5 mL microfuge tube, 1 ml of Tris- Reagent was added. This mixture was vortexed for 30-45 seconds. The homogenate was centrifuged at 10000 g for 5 minutes at 4^{0}C. The supernatant was collected in a fresh tube and ¼ volume of chloroform was added, vortexed well, and kept on a rocker at room temperature for 15 minutes to mix. The tube was then centrifuged at 10000 g at 4^{0}C for 10 minutes and 750 µL of the upper aqueous layer was collected into a fresh tube. RNA was precipitated by adding 500 mL of isopropanol, and centrifugation at 10000 g for 10 minutes at 4^{0}C. RNA pellets was washed with 500 µL 70% ice-cold ethanol and centrifuged at 10000 g for 5 minutes at 4^{0}C. Pellet was air dried and suspended in 60 µL DEPC- treated water and stored at -80^{0}C until further use.

1.2. For cDNA synthesis, RNA samples were treated with, DNase I (NEB) per manufacturer's instructions to remove DNA contaminations. RNA samples were then reverse transcribed into cDNA (complementary DNA) using the M-MuLV RT enzyme (NEB) per manufacturer's directions and the cDNA samples were stored at -

80^0C until future use. For qPCR and RT-PCR experiments, 1:50 dilution in Millipore filtered water was used.

Semi-quantitative Reverse Transcription-PCR (RT-PCR) analysis

To test relative gene expression, cDNA samples formulated from extracted RNA were used as template DNA in PCR reactions. The concentration of template cDNA was normalized by amplifying Tubulin A (*TUA*) as the reference gene. To ensure equalized bands were not saturated, both reference and target genes were amplified at least two different number of cycles.

Quantitative Real-Time PCR (qRT-PCR) analysis

qRT-PCR was used to analyze the transcript levels of cDNA samples with SYBR® Green using the Bio-Rad CFX Connect Real-Time System according to the manufacturer's instructions. The PCR program used was as follows: 55^0C for 2 minutes, 95^0C for 10 minutes, then 40 cycles of 95^0C for 25 seconds and 62^0C for 20 seconds. The averages of three technical replicates were analyzed using the ΔCT method [35]. The relative expression of the genes was normalized against *TIP41* reference gene. Primers used for this analysis are listed in Table 1.

Genotyping of mutants and transgenic lines

To genotype *nrpb4* mutants (T-DNA insertional mutant), a fragment of genomic DNA was amplified followed by agarose gel electrophoresis. The DNA samples which did not show any bands with the *nrpb4* gene specific forward and reverse primers (Table-I) were selected and the DNA was amplified using T-DNA left border sequence specific primer and *nrpb4* gene specific reverse primer.

The transgenic lines used in this research were genotyped using antibiotic resistance present within the transgenes. Seeds from transgenic lines were screened on the ATS medium containing the respective antibiotics specific for the transgene present. *35S::NRPB4-HA* and *35S::HA-NRPB4* lines were screened on kanamycin (50 µg/ml) and hygromycin (16 µg/ml); *35S::IBR5-Myc* line was screened on kanamycin (50 µg/ml).

Cloning and plasmid manipulation

1.1.Cloning-The gene of interest was amplified using the cDNA library, CD4-7 Newman Lambda PRL2 (ABRC) and gene specific primers residing the restriction sites within them were used for same. The gene was amplified by PCR with the Phusion Taq polymerase (NEB). The amplified fragment was purified as described in the agarose gel purification kit (MoBio Laboratories, Inc) assessed by gel electrophoresis to confirm the purification and the purified DNA was stored at -20^{0}C.

1.2.Plasmid DNA isolation- The *E. coli* host carrying the vector into which the gene was to be cloned was cultured at 37^{0}C at 200 RPM overnight in liquid LB medium with the specific antibiotic for the bacterial resistance. Plasmid DNA was isolated as previously described [55].

The plasmid DNA was digested using appropriate restriction enzymes and gene of interest was ligated to the vector.

1.3.Transformation- The vector carrying the gene of interest was transformed into *E. coli* host cells (Top 10) by $CaCl_2$ or by electroporation. The transformed cells were plated on to solid LB medium with the specific antibiotics. The LB plates were stored at 37^{0}C overnight to select the positive colonies and confirmed through colony PCR and restriction digestion.

To produce GST fusion protein constructs, the coding sequences from CD4-7 Newman Lambda PRL2 cDNA library (ABRC) was amplified. *NRPB4* cDNA was amplified using the gene specific primers, RPB4-EcoRI-F and RPB4-SalI-R (Table 1), and Phusion high fidelity DNA Polymerase (NEB). *NRPB4* deletion constructs were generated as follows: for C-terminal deletion of *NRPB4* (0-168bp region), gene specific primers RPB4- EcoRI-F and NRPB4- RD1 were used; for N-terminal deletion of *NRPB4* (146-417bp region), gene specific primers NRPB4- FD1 and RPB4-SalI-R were used; and for *NRPB4* mid region (74-244bp region) gene specific primers NRPB4- MR-F and NRPB4- MR-R were used. The coding sequence of the full length *NRPB4* and deletions were first ligated into the *EcoRV* site of the pBlueScript II SK (-) (Stratagene) cloning vector, and then ligated into *EcoRI- SalI* site of pGEX4T-3 (Pharmacia) expression vector. The expression vector with the clones were transformed into BL21-DE3 *E. coli* cells.

Expression of protein in bacteria

1.1.For *E.* coli cultures, liquid LB medium with Carbenicillin (100µg/ml) with the inoculant from bacterial culture (glycerol stock) was used to for the expression of protein in bacteria. This culture was grown overnight at 37^0C; 200 rpm in a rotary shaker. The overnight culture was inoculated into 250 ml of liquid LB medium with carbenicillin at 100µg/ml and incubated at 37^0C; 200 rpm in an incubator till the OD reached 0.6. The culture was then induced using 2mM final concentration of IPTG (Gold Biotechnology) and incubated at 30^0C; 200 rpm for 5-6 hours. The bacterial cells were then obtained by centrifuging the culture at 10000 g for 10 minutes and the bacterial pellet was stored at -80^0C.

1.2.For *Agrobacterium* cultures, liquid LB medium with rifampicin (50µg/ml) and gentamycin (25µg/ml) with the pertinent inoculant from bacterial culture (glycerol stock) was used. The culture was grown at 30^0C; 200 rpm for 36 hours and the same was used to upscale to a larger volume of culture with liquid LB medium having rifampicin (50µg/ml) and gentamycin (25µg/ml). The culture was incubated for 36 hours at 30^0C; 200 rpm. The culture was centrifuged at 12,500 rpm for 10 minutes and the bacterial pellet was used in transformation of *A. thaliana* plants by floral dip method as previously described [29].

To generate stably expressed Arabidopsis HA-NRPB4 in wild-type and IBR5-Myc backgrounds, RPB4 EcoR1-F and RPB4 Sal1-R primers were used for the amplification which generated blunt-end products and were inserted into a Directional TOPO vector (Invtrogen), pENTR/SD/D- TOPO and transformed into *E. coli* host cells- TOP10. The purified plasmid was digested using *Mlu1* restriction enzyme (New England BioLabs). Using Gateway LR Clonase (Invitrogen) recombination reaction was done to insert *NRPB4* clones into the pEarleyGate 201 (ABRC) expression vector. The plasmid was transformed into *E. coli* TOP10 cells and then purified and transformed by electroporation into *Agrobacterium tumefaciens* GV3101 competent cells.

Protein expression and purification

To analyze the GST-fusion purified proteins, GST-NRPB4 pellet stored at -80^0C and resuspended on ice in 6ml 1X phosphate buffered saline (PBS) containing 2.7mM KCl; 137mM NaCl; 2mM KH_2PO_4 pH 7.4; 10mM NaH_2PO_4. The bacterial cells were lysed by sonicating 4 times for 15 seconds, with 10 seconds intervals on ice in between each

sonication. To the cell lysate, 1mM phenylmethylsufonyl fluoride (PMSF, Amresco) and 0.1% Tween-20 (Sigma) were added and the solution was kept on a rocker at 4^0C for 10 minutes. It was then centrifuged for 10 minutes at 10000 g at 4^0C and the supernatant was collected in a fresh tube to which 30-40 µL of Glutathione beads were added. The tube was kept on a rocker at 4^0C overnight. Beads were washed 3 times for 10 minutes each wash with 1X PBS+ 0.1% Tween-20 and the beads were resuspended in 40-60µL 1X PBS and stored at 4^0C.

For plant derived IBR5-Myc protein interaction assay, 10 day-old transgenic seedlings expressing IBR5-Myc were homogenized in native extraction buffer containing 50mM Tris-Cl (pH- 7.2); 10% glycerol; 4mM EGTA; 100mM NaCl; 0.1% Tween-20; 1mM PMSF; complete mini protease inhibitor cocktail (Roche Diagnostics) and; 10µm MG-132 [8]. The cell lysate was kept on rocker for 10 minutes at 4^0C and centrifuged at 10000 g for 10 minutes at 4^0C. The supernatant was collected in a fresh tube to estimate the concentration of total protein as previously described [30], and 1ml aliquots of the protein extracts was stored at -80^0C.

***In-vitro* protein-protein interaction**

GST-NRPB4 (10µL) conjugated to glutathione- agarose beads were incubated with IBR5-Myc plant extracts (600-1000µg) at 4^0C for 4 hours with gentle agitation. The extract was discarded, and beads were washed for a total of 4 times for 10 minutes at 4^0C with washing buffer containing 50mM Tris-Cl (pH- 7.2); 10% glycerol; 4mM EGTA; 100mM NaCl; 0.1% Tween-20; 1mM PMSF in the first wash and the same buffer without 4mM EGTA was used to further wash the beads for 3 more times. The beads were resuspended in 2X Laemmli sample buffer consisting 40 g/L SDS; 250mM Tris-Cl

(pH- 6.8); 20% glycerol; 10% β- mercaptoethanol (v/v) and; 30 g/L bromophenol blue for SDS-PAGE.

***In-vivo* protein-protein interaction**

For Co-immunoprecipitation assay, 10-day-old seedlings of IBR5-Myc and HA-NRPB4 in IBR5-Myc were homogenized in native extraction buffer as mentioned above. The total protein concentration of the extract was equalized after the Bradford assay and the extracts were incubated with anti- HA agarose beads (Roche) for 4 hours with gentle agitation at 4^0C. The beads were washed 4 times with wash buffer consisting of 50mM Tris-Cl (pH- 7.2); 10% glycerol; 4mM EGTA; 100mM NaCl; 0.1% Tween-20 and resuspended in 2X LSB.

Protein separation by SDS-PAGE and western blot analysis

12.5% polyacrylamide gels were used for SDS-PAGE. The samples were loaded in the gel after it was boiled in 2X LSB to denature and elute the proteins for 7 minutes. Bio-Rad Mini- PROTEAN II Cell was used to set-up the gel electrophoresis. For molecular weight standard, Page Ruler Plus Protein Ladder (Thermo Scientific) was used. The gel was run at 90V for 15 minutes until the dye reached the separating gel and the voltage was increased to 160V and further run for 60-75 minutes.

For western blot analysis, proteins were transferred by wet electro-transfer (90V for 1 hour 30 minutes) on to PVDF membrane (Bio-Rad). The membrane was then blocked using 5% w/v non-fat dry milk in TBST (Tris buffered saline) containing 150 mM NaCl; 50 mM Tris-Cl (pH- 7.5); and 0.1% Tween-20 for at least 1 hour at room temperature. The membrane was washed in TBST 3 times for 5 minutes and membrane was incubated in 1:10,000 dilution the primary antibody (anti-Myc or anti-HA) for 2.5

hours to overnight (4^0C if overnight) with gentle rocking. The membrane was washed 3 times for 5 minutes with TBST and incubated with secondary antibody (Mouse IgG) for 1 hour at room temperature with gentle rocking. The membrane was washed once for 15 minutes, and 3 times for 7 minutes with TBST. The targeted proteins were observed via X-ray film exposure using Bio-Rad Clarity Western ECL Substrate (chemiluminescent substrate).

Root growth and hypocotyl elongation assays

For auxin supplemented root growth assay, 4 days-old *nrpb4* mutant and Col-0 seedlings germinated and grown on ATS (1% sucrose) under continuous light condition were transferred on to fresh plates containing ATS (1%) + specific concentration of auxin IBA, IAA, Picloram or 2,4-D. A line was drawn on the plates and the root tip of the seedlings were placed on the line and further incubated for 2 days. The length of the root grown past the line drawn was measured to the closest mm to calculate the percent root growth inhibition between genotypes in comparison with the control. The assay was conducted at least 3 times with a sample size of 15 seedlings.

For heat stressed root growth and hypocotyl elongation assay, the seeds of heterozygous *nrpb4* mutants and Col-0 were germinated and grown on ATS (1%) for 4 days. The seedlings were transferred on to fresh plates containing ATS (1%) and the root tip or the hypocotyl was placed on the line drawn on the plate as mentioned above. The plates were incubated at 22^0C or 30^0C for 2 more days under continuous light condition and the root length and hypocotyl elongation past the line drawn was measured and percent inhibition was calculated as mentioned above.

Histochemical staining of GUS proteins

The *IBR5::IBR5.1-GUS* was previously described (Dharmasiri et al. 2014). Seedlings expressing *IBR5::IBR5.1-GUS* was grown on ATS (1%) media for 4 days before staining and it was place in fixer solution [10mM 2-(N-morpholino) ethane sulfonic acid (MES), 0.3M mannitol, 0.3% formaldehyde] and vacuum infiltrated for 10 minutes. The seedlings were then gently rocked at room temperature for 30 minutes, washed by gently rocking in phosphate wash buffer [100mM Na2HPO4, pH 7.0] 3X for 5 minutes. Seedlings were stained with staining solution [100mM Na2HPO4 (pH 7.0), 1 mM potassium ferricyanide, 1 mM potassium ferrocyanide, 0.1M 5-Bromo-4-chloro-3-indoxyl-beta-D-glucuronide cyclohexyl ammonium salt, 10mM EDTA, 0.1% Triton X-100 (v/v)] by vacuum infiltrating for 15 minutes as described by Jefferson (1987). The seedlings were then kept at 37^0C in darkness for 16 hours to develop blue color.

Data analysis

The root length and hypocotyl elongation were measured using ImageJ software and the average percent root growth inhibition was calculated using the formula:

$$\text{Percent (\%) root growth} = \frac{\sum \left[\frac{(\text{average control length}) - (\text{average treated length})}{(\text{average control length})} * 100 \right]}{n}$$

Error bars in all graphs illustrates either standard deviation or standard error of the mean, calculated as follows:

$$\text{Standard deviation } (\sigma) = \sqrt{\frac{\sum (x - \bar{x})^2}{n}}$$

$$\text{Standard error} = \frac{\text{Standard deviation}}{\sqrt{n}}$$

The data was analyzed by ANOVA using Vassar Stats: Website for Statistical Computation (http://vassarstats.net/).

Table 1. Primer sequences

Primer Name	Primer Sequence	Primer Length	Tm (^{0}C)
NRPB4-FP	5'CAGCCGCTACAAGAATCCAGATGCTGTT3'	28	84
NRPB4-RP	5'CTCGAATCTCTTGACAAGTGAGAG3'	24	70
RPB4-EcoR1-F	5'TTGAATTCCACCATGTCCGGAGAAG3'	25	72
NRPB4-Rd1 (Sal1)	5'GCGTCGACTACTCAAACACTTGAGAAACTT3'	30	86
NRPB4-Fd1 (EcoR1)	5'GAGAATTCGAATCAAGTTTCTCAAGTG3'	27	74
RPB4-Sal1-R	5'CTTGAGAGTCGACTGCACTACTCG3'	24	75
NRPB4-MR-EcoR1-FP	5'ATGAATTCTGAATTCTCTTTGATTCTTGAG3'	30	72
NRPB4-MR-Sal1	5'CTAATGTCGACTTAGTATTTCTCGAACTTGTCTAAC3'	33	86
NRPB4-BiFC-EcoR1-N-tag-FP	5'AAGGCGAATTCTTCCGGAGAAGAAGAAGAGAACGC3'	35	65
NRPB4-BiFC-BamH1-N-tag-RP	5'AAGGGATCCCTCGAATCTCTTGACAAGTGAGAGAT3'	35	64
NRPB4-BiFC-EcoR1-C-tag-FP	5'GGCGAATTCTCCGGAGAAGAAGAAGAGAACGC3'	32	65
NRPB4-BiFC-BamH1-C-tag-RP	5'CCGGATCCACTCGAATCTCTTGACAAGTGAGAG3'	33	64
IBR5 Kpn1 no start-F*	5'GCAGGTACCAGGAAGAGAGAAAGAGAGAACCCT3'	33	65
IBR5 BamH1 no stop- R*	5'TTAGGATCCAGAGCCATCCATTGCAATATCACCA3'	34	64
IBR5 Kpn1+2 no start- F*	5'GCAGGTACCAGAGGAAGAGAGAAAGAGAGAACCCT3'	35	65
IBR5+1 BamH1 no stop- R*	5'TTAGGATCCTAGAGCCATCCATTGCAATATCACCA3'	35	63
LBO2***	5'TTGGGTGATGGTTCACGTAGTGGGCC3'	26	65
TUA F**	5'GCAGCTATCAGTCCCTGAGATC3'	22	68
TUA R**	5'TCCACCTTCAGCACCAACTTCT3'	22	68

*****Designed by Timothy Cioffi

**Designed by Sunethra Dharmasiri

***Designed by Salk Institute

III. RESULTS

IBR5 interacts with AtNRPB4 *in-vitro*

To confirm yeast two-hybrid assay results, an *in vitro* pull-down assay was performed. This was achieved by incubating bacterially expressed GST-NRPB4 with protein extract from Arabidopsis plants overexpressing IBR5-Myc. An anti-Myc western blot analysis revealed that GST-NRPB4 specifically pulled down IBR5-Myc [Figure 5].

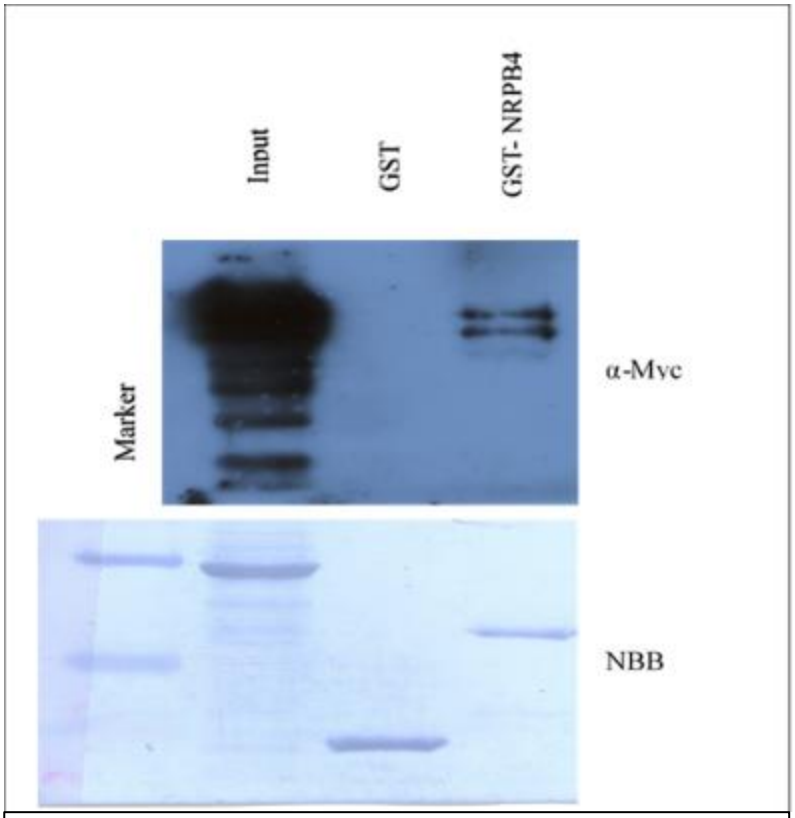

Figure 5. In vitro interaction between *NRPB4* and *IBR5.* Bacterially expressed GST and *GST-NRPB4* proteins were isolated using glutathione- agarose beads and added to crude protein extract from Arabidopsis plant expressing *IBR5-Myc. GST-NRPB4* interacting proteins were pulled down using glutathione beads and an anti-Myc western analysis was performed

There are several putative domains in both IBR5 and NRPB4 that could be necessary for the IBR5-NRPB4 interaction. IBR5 has an F-box like domain (located on the N-terminus), a catalytic domain, and a calmodulin binding domain. *NRPB4* has conserved N-terminal and C-terminal regions that are involved in protein-protein interactions [14].

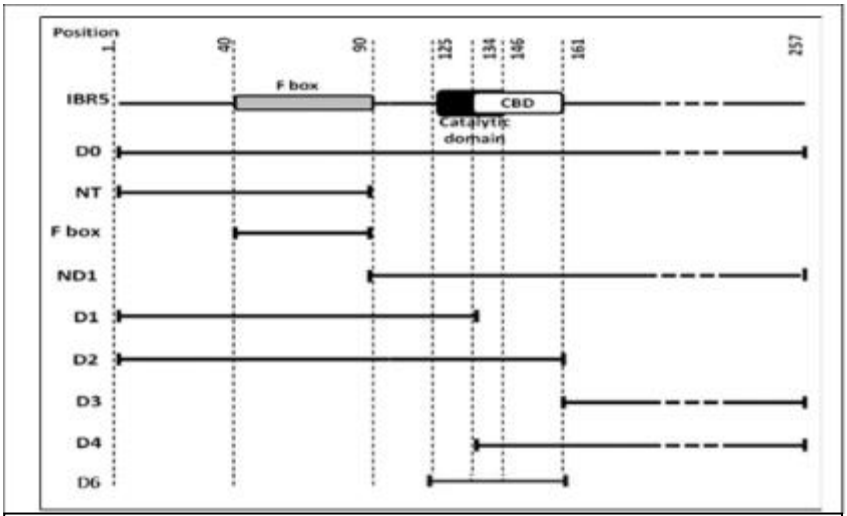

Figure 6. Deletion constructs of *IBR5.*
Recombinant protein fragments are tagged with Myc and the Calmodulin Binding Domain (CBD) is denoted in full length protein.

To determine the interacting domains, a series of pulldown assays were done with various IBR5 and NRPB4 deletion constructs. Myc-tagged recombinant truncated peptides of IBR5 expressed in *E. coli* [Figure 6] were incubated with GST-NRPB4 protein, pulled down with glutathione-agarose beads, and analyzed using anti-Myc antibody. Results indicate that NRPB4 interacts with truncated IBR5 with the Calmodulin Binding Domain (CamBD) and catalytic domain, specifically ND1, D0, D2 and D6 deletion constructs [Figure 7].

Since CBD of IBR5 is involved in the interaction with NRPB4 and IBR5 has been previously shown to interact with Ca^{2+}/CaM, the effect of Ca^{2+} on IBR5-NRPB4 interaction was tested. A pull-down assay was performed using bacterially expressed GST-NRPB4 and protein extracted from Arabidopsis seedlings expressing *35S::IBR5-Myc*. An anti-Myc western blot analysis revealed that IBR5-Myc and GST-NRPB4

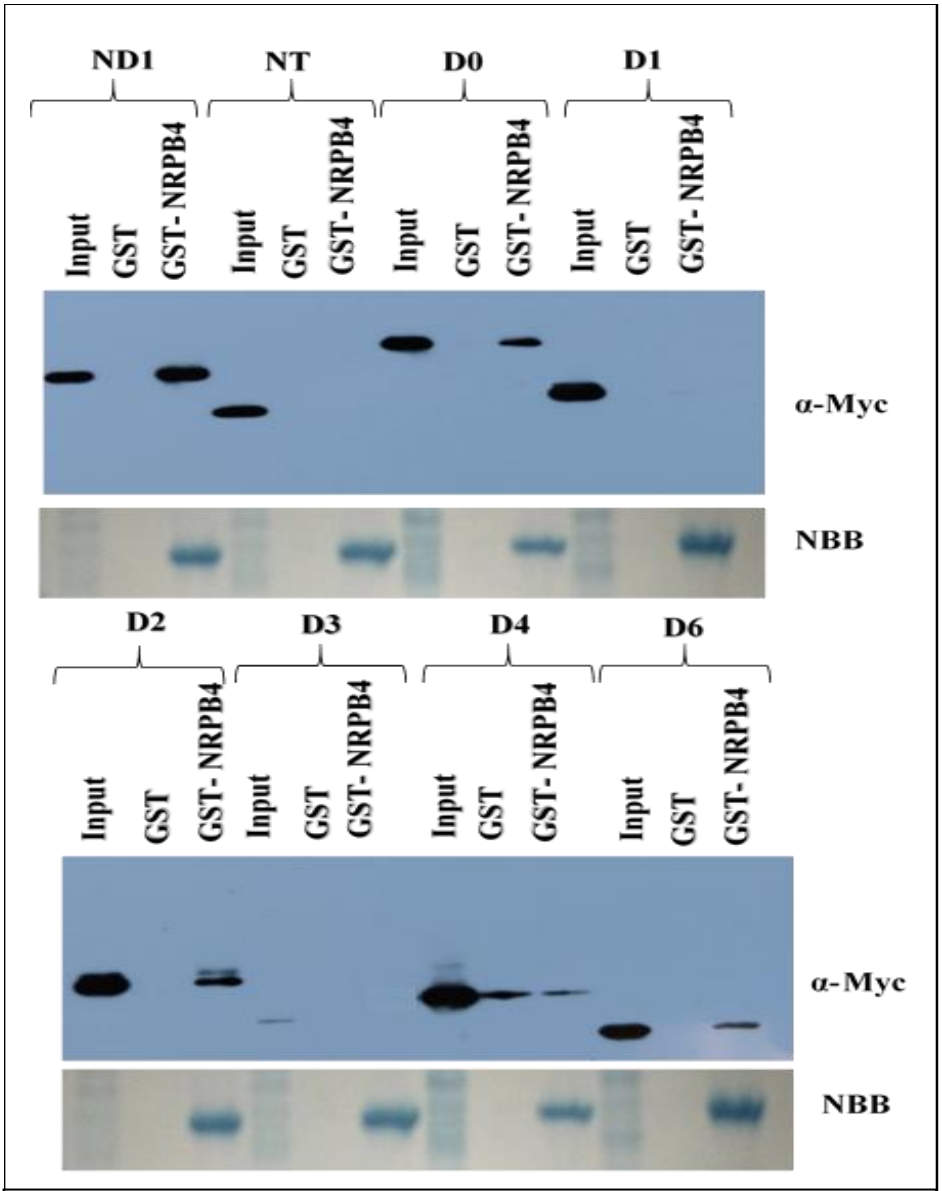

Figure 7. In vitro interaction between NRPB4 and *IBR5*.
Bacterially expressed GST, *GST-IBR5* (deletion constructs) and *GST-NRPB4* protein were isolated using glutathione- agarose beads.

interaction was considerably enhanced when Ca^{2+} ions are chelated with EGTA [Figure 8].

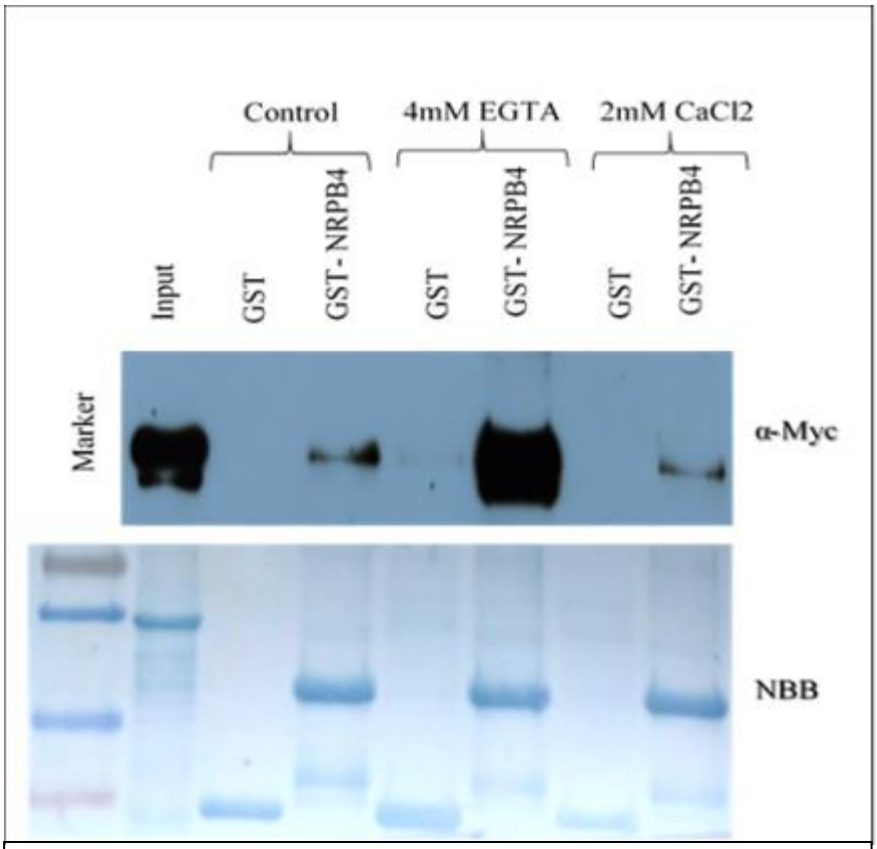

Figure 8. In vitro interaction between NRPB4 and *IBR5*. Bacterially expressed GST and *GST-NRPB4* protein were isolated using glutathione-agarose beads and added to native protein extract from transgenic Arabidopsis plant expressing *35S::IBR5-Myc*. *GST-NRPB4* interacting proteins were pulled down using glutathione beads in the presence or absence of Ca^{2+} ions and an anti-Myc western analysis was performed.

Furthermore, it has been shown in yeast that RPB4 has conserved N- and C-termini regions and are involved in protein-protein interaction with RPB7 [24]. To determine NRPB4 interacting regions with IBR5, deletion constructs of NRPB4 were made [Figure 9a], tagged with GST and expressed in *E. coli* cells. A pull-down assay was performed using plant derived *IBR5-Myc* crude extract and bacterially expressed GST-NRPB4, GST-NRPB4-CTD, GST-NRPB4-MR and GST-NRPB4-NTD bound to

glutathione beads. An anti-Myc western analysis revealed that IBR5 interacted with both N- and C-termini of NRPB4 [Figure 9b], suggesting the presence of the conserved regions on N- and C- termini in Arabidopsis involved in interaction with IBR5.

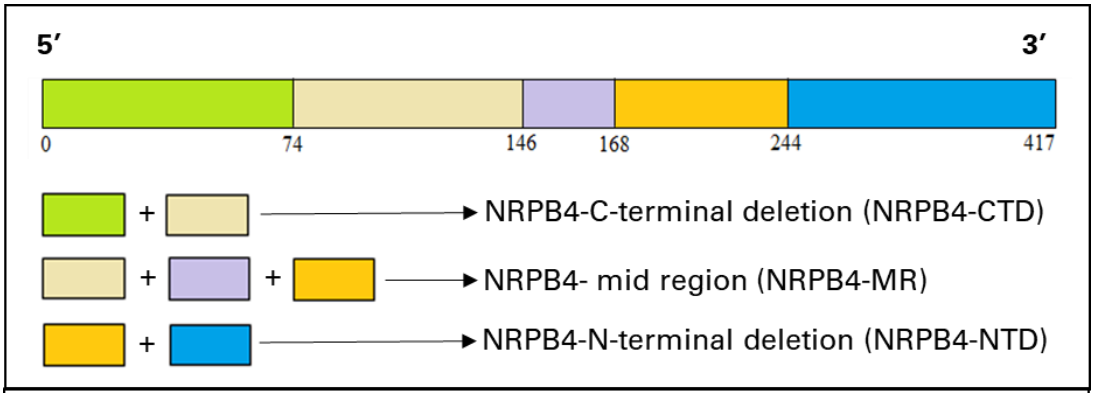

Figure 9a. Deletion constructs of *NRPB4*.
Recombinant protein fragments are tagged with GST and expressed in *E. coli* cells.

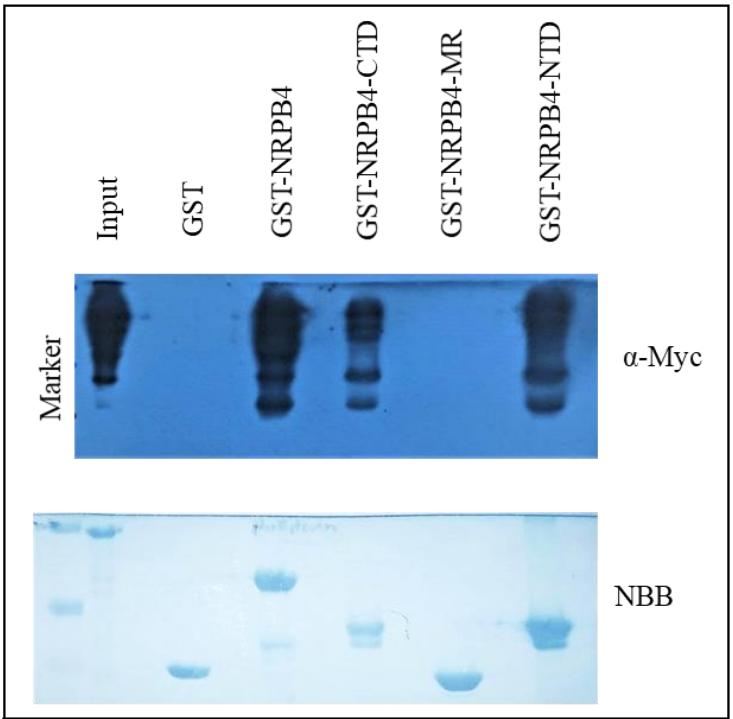

Figure 9b. . In vitro interaction between *NRPB4* (deletion constructs) and *IBR5*.
A pull-down assay was performed using plant derived *IBR5-Myc* crude extract and bacterially expressed *GST-NRPB4, GST-NRPB4-CTD, GST-NRPB4-MR* and *GST-NRPB4-NTD* bound to glutathione beads. An anti-Myc western analysis was performed.

Interestingly, GST-NRPB4-MR region was found to be smaller in size than GST itself. The construct was confirmed by EcoRI and SalI digestion and PCR using NRPB4-MR-EcoRI-FP and NRPB4-MR-SalI-RP primers (Table 1). This might be due to the change in conformation of the protein when tagged with GST.

***nrpb4* homozygous mutants show pleotropic developmental defects.**

A T-DNA insertional mutant was obtained from Arabidopsis Biological Resource Center (ABRC) and homozygous *nrpb4* mutant was identified. *nrpb4* mutants exhibit severe growth retardation under normal growth conditions [Figure 10], and hardly produce seeds.

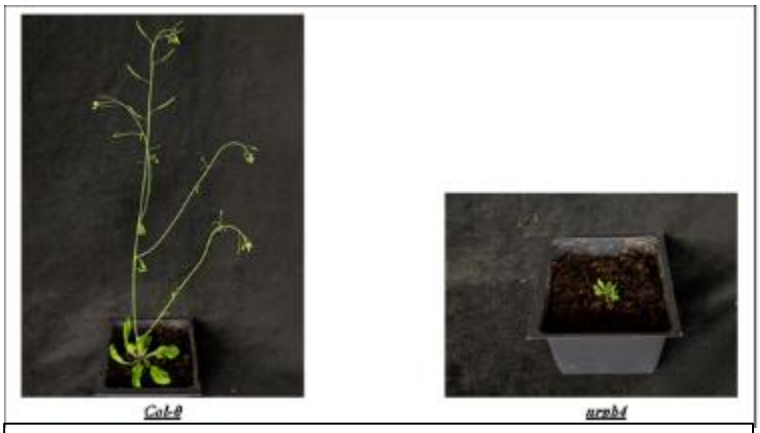

Figure 10. 4-week-old *nrpb4* mutant plant shows growth defects.
Col-0 and *nrpb4* mutant were grown on ATS and 10-day-old seedlings were transferred to soil. Images taken was of four-week-old plants

***nrpb4* shows defect in auxin/ high- temperature responses.**

Previous studies have shown an enhanced root and hypocotyl elongation in wild-type plants in response to higher temperature [27]. Since previous studies in yeast have shown that NRPB4 orthologs are important in responding to the high temperature, *nrpb4*

primary root length and hypocotyl elongation were compared with the wild type Col-0. The Col-0 and *nrpb4* mutants were grown on ATS at 22^0C for four days and then incubated at ambient and high temperature (22^0C and 30^0C respectively). The root length was measured after 2 days of incubation at respective temperatures. The result shows that there was a significant difference between the wild type and *nrpb4* mutants at both

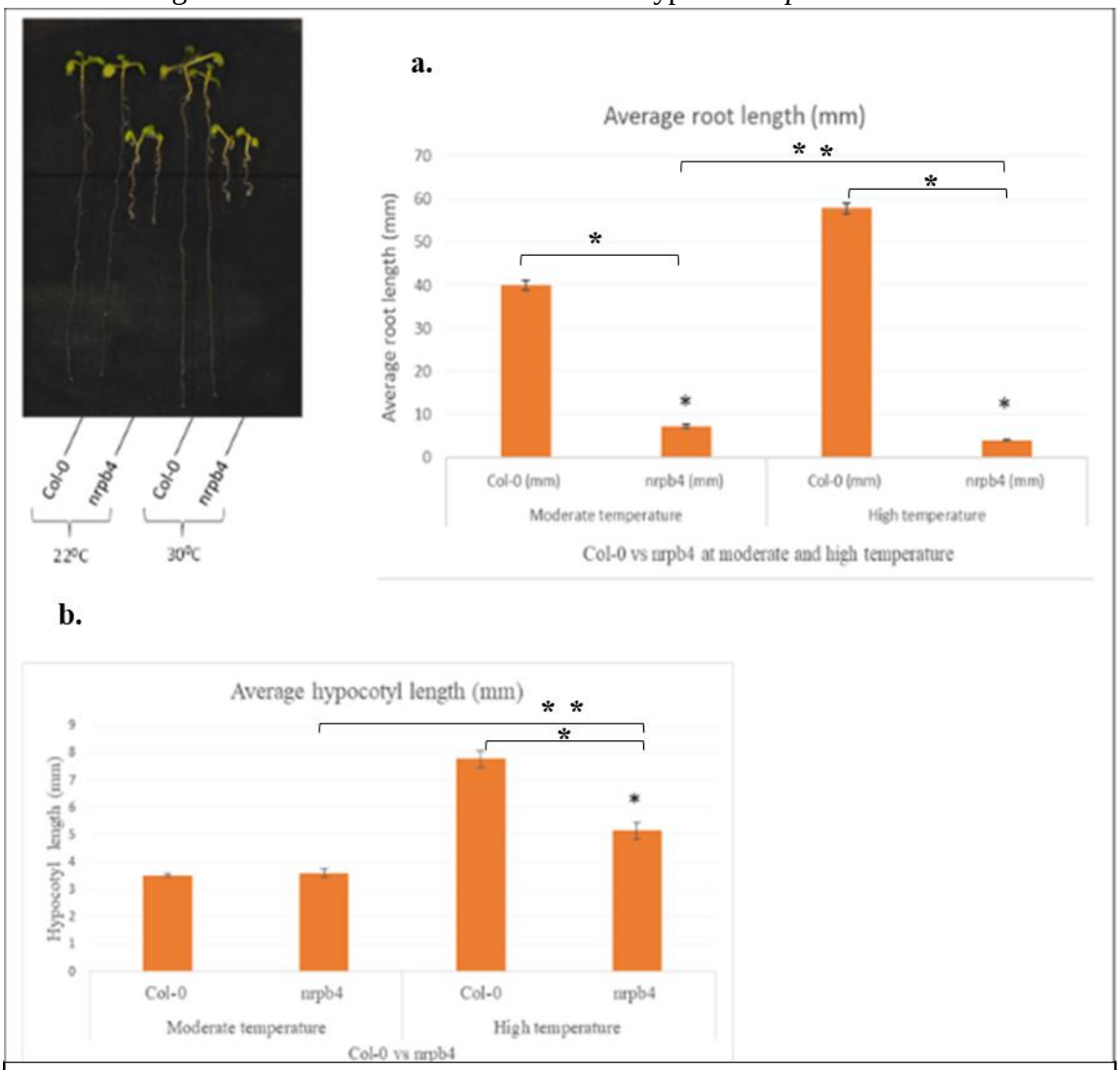

Figure 11. Col-0 and *nrpb4* mutants show root growth defects at moderate and high temperature.
Col-0 and *nrpb4* mutants grown on ATS (1%). The four-day old seedlings were transferred to 22^0C and 30^0C and incubated for two days. The root and hypocotyl length were measured using ImageJ and the data was analyzed using ANOVA. **(* indicates significance mean difference between *nrpb4* and wild-type and ** indicates significance mean difference between each other; where P >0.001).**

ambient and high temperature, suggesting an overall root growth defect of the *nrpb4* mutants [Figure 11].

Additionally, results also show that *nrpb4* is defective in high temperature induced hypocotyl elongation probably due to a defect in auxin response.

Since the mutants showed defective response to temperature induced hypocotyl elongation is linked to auxin response [51], the auxin response of *nrpb4* mutant was tested using root growth analysis. The primary root growth of Col-0 and *nrpb4* was compared on auxin supplemented media using Indole-3- Acetic Acid (IAA), Indole- 3-Butyric Acid (IBA), 2,4-Dichlorophenoxyacetic acid (2,4-D) and Picloram.

The root growth inhibition assays on different auxin supplemented vs. unsupplemented media indicate that *nrpb4* mutant is significantly insensitive to IAA, 2,4-D, IBA and Picloram [Figure 12 to Figure 19] suggesting that auxin response pathway has been affected in *nrpb4*. Interestingly, on IAA supplemented medium, the root growth

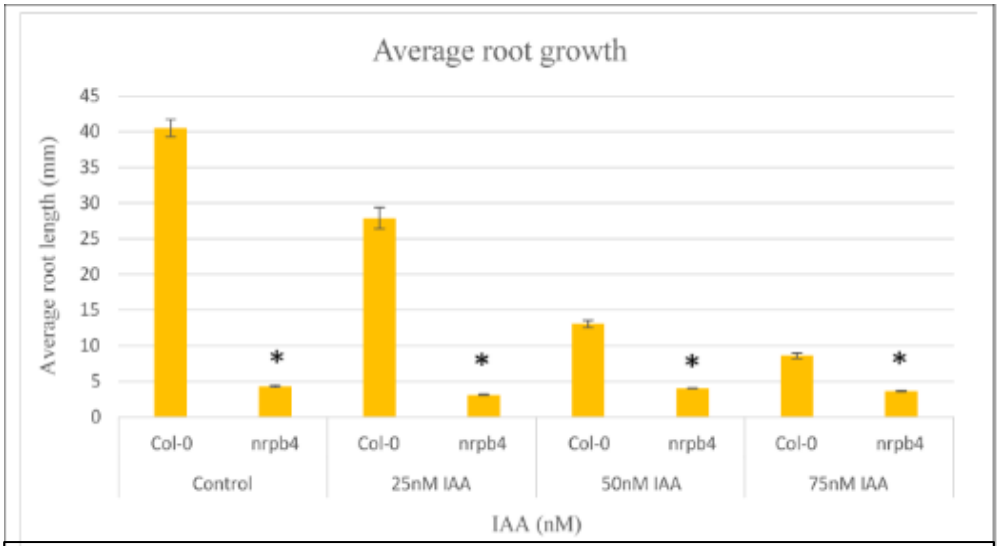

Figure 12. nrpb4 mutant showing resistance to auxin IAA.
Col-0 and *nrpb4* mutant grown on ATS (1%). The four-day old seedlings were transferred on to IAA (25nM; 50nM and 75nM) and incubated for two days. The average root length was measured using ImageJ and the data was analyzed using ANOVA. **(* indicates mean differ significantly from wild-type; P>0.001).**

inhibition on 25nM IAA was more when compared to 50nM and 75nM IAA respectively. This could be the case as 25nM IAA was optimum concentration to be used.

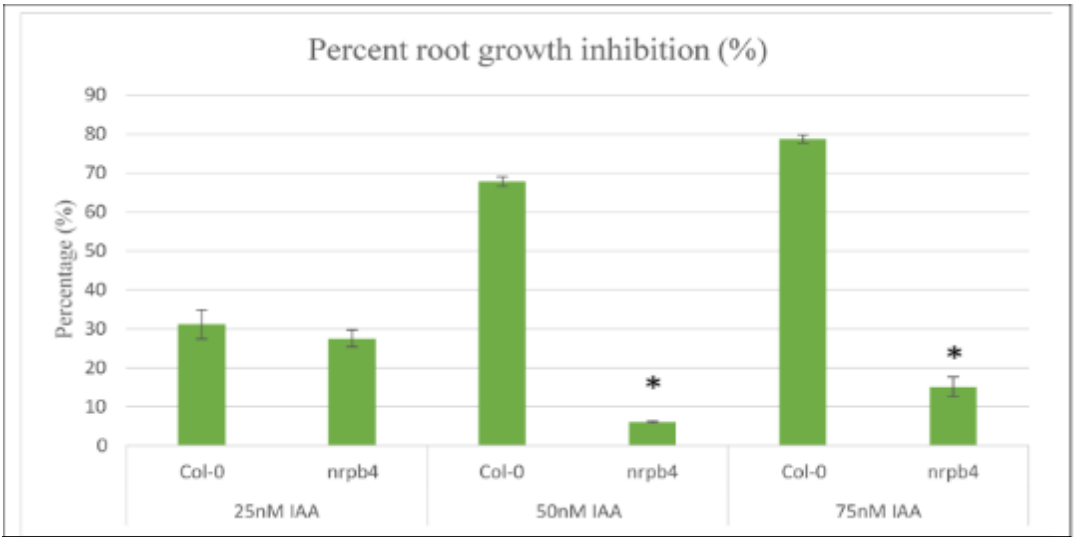

Figure 13. nrpb4 mutant showing resistance to auxin IAA.
Col-0 and *nrpb4* mutant grown on ATS (1%). The four-day old seedlings were transferred on to IAA (25nM; 50nM and 75nM) and incubated for two days. The percent root growth inhibition was calculated, and the data was analyzed using ANOVA. **(* indicates mean differ significantly from wild-type; P>0.001).**

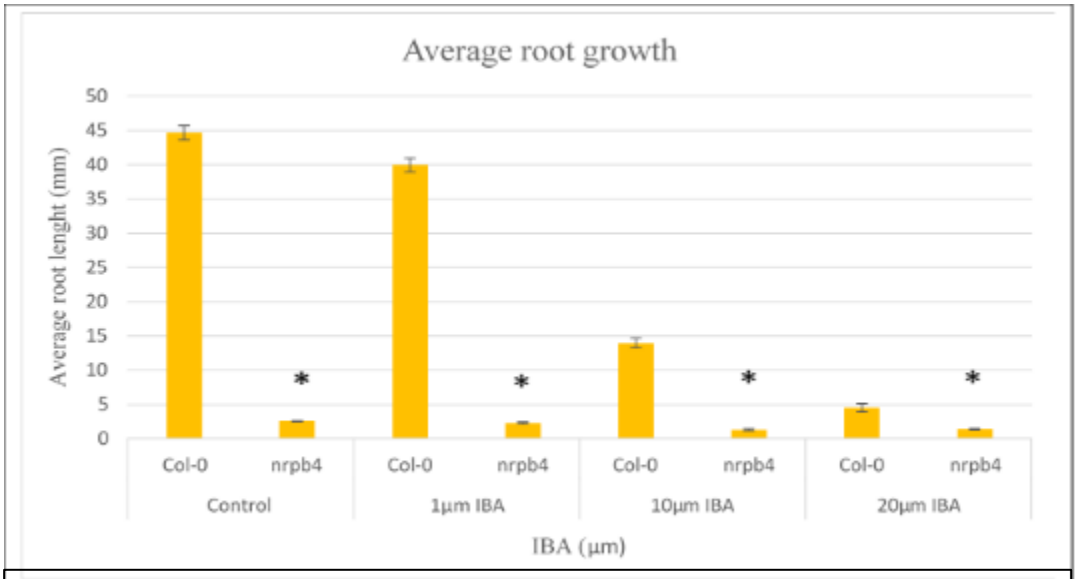

Figure 14. nrpb4 mutant showing resistance to auxin IBA.
Col-0 and *nrpb4* mutant grown on ATS (1%). The four-day old seedlings were transferred on to IBA (1µM; 10µM and 20µM) and incubated for two days. The average root length was measured using ImageJ and the data was analyzed using ANOVA. **(* indicates mean differ significantly from wild-type; P>0.001).**

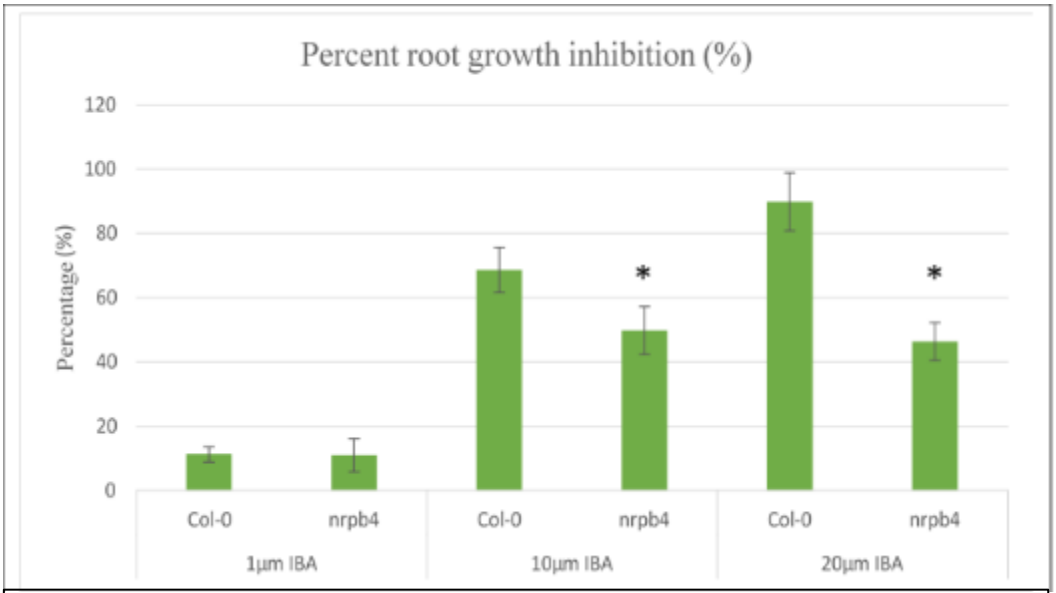

Figure 15. nrpb4 mutant showing resistance to auxin IBA.
Col-0 and *nrpb4* mutant grown on ATS (1%). The four-day old seedlings were transferred on to IBA (1µM; 10µM and 20µM) and incubated for two days. The percent root growth inhibition was calculated, and the data was analyzed using ANOVA. **(* indicates mean differ significantly from wild-type; P>0.001).**

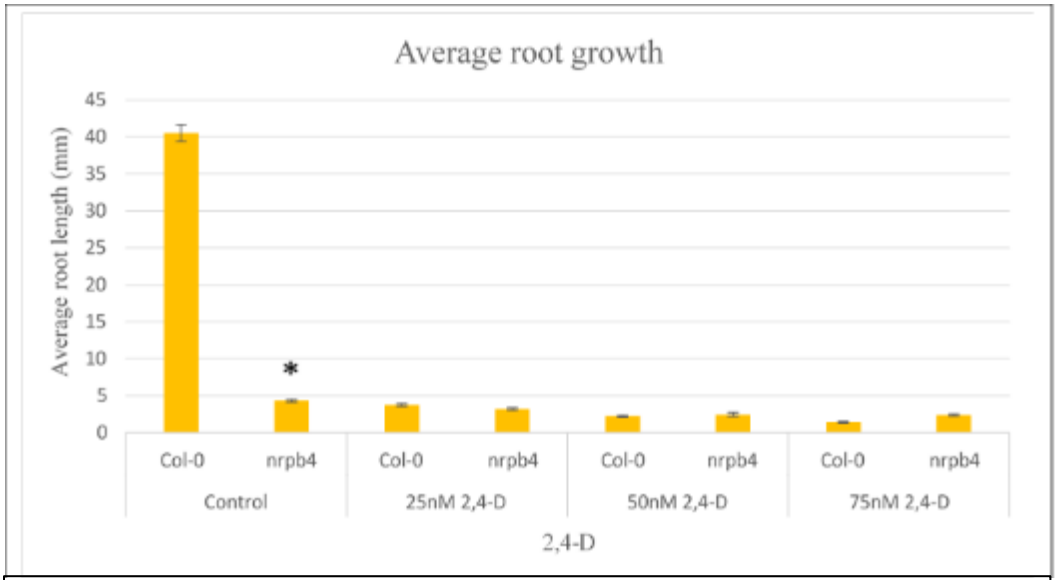

Figure 16. nrpb4 mutant showing resistance to auxin 2,4-D.
Col-0 and *nrpb4* mutant grown on ATS (1%). The four-day old seedlings were transferred on to 2,4-D (25nM; 50nM and 75nM) and incubated for two days. The average root length was measured using ImageJ and the data was analyzed using ANOVA. **(* indicates mean differ significantly from wild-type; P>0.001).**

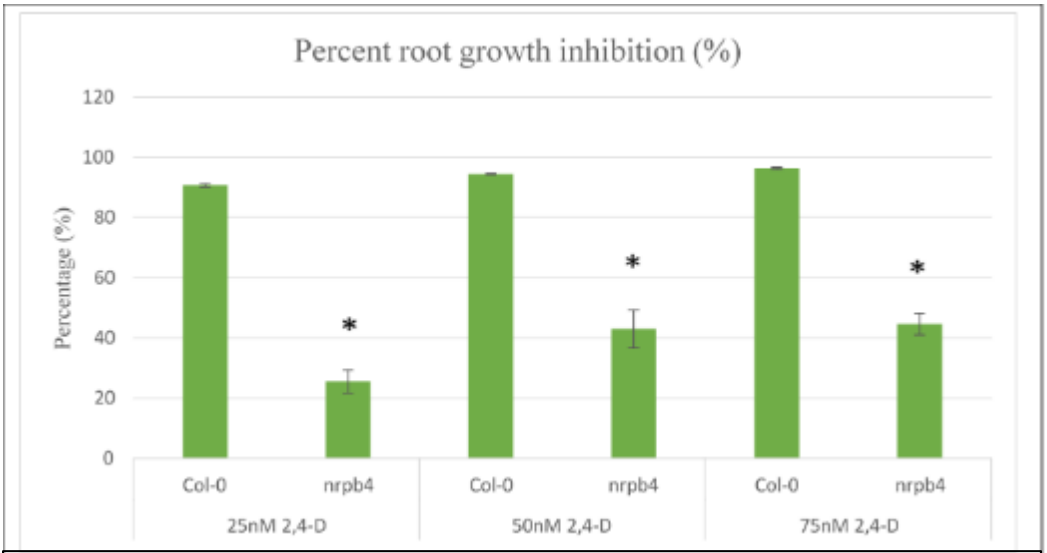

Figure 17. nrpb4 mutant showing resistance to auxin 2,4-D.
Col-0 and *nrpb4* mutant grown on ATS (1%). The four-day old seedlings were transferred on to 2,4-D (25nM; 50nM and 75nM) and incubated for two days. The percent root growth inhibition was calculated, and the data was analyzed using ANOVA. **(* indicates mean differ significantly from wild-type; P>0.001).**

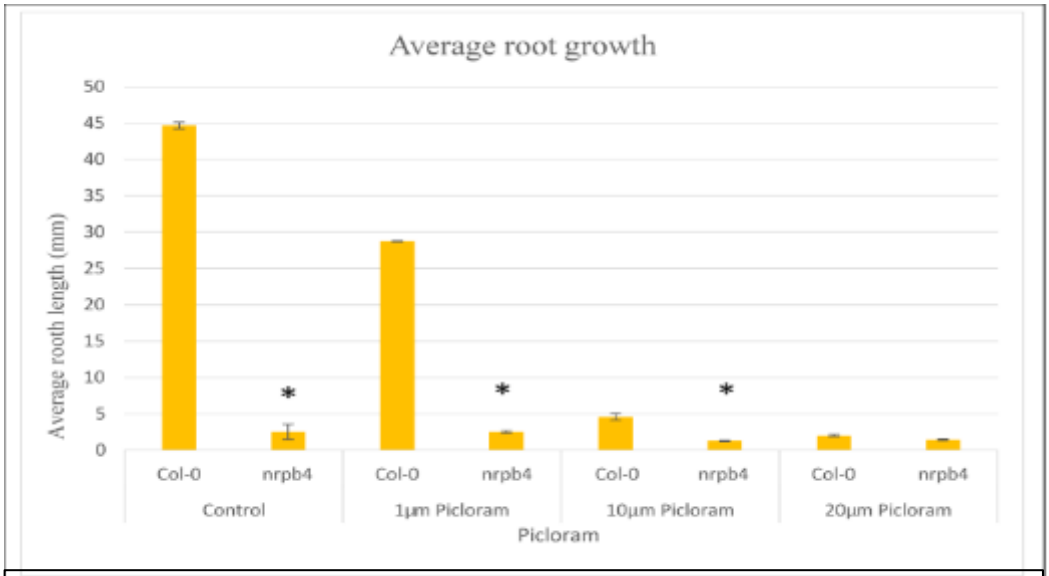

Figure 18. nrpb4 mutant showing resistance to auxin Picloram.
Col-0 and *nrpb4* mutant grown on ATS (1%). The four-day old seedlings were transferred on to Picloram (1µM; 10µM and 20µM) and incubated for two days. The average root length was measured using ImageJ and the data was analyzed using ANOVA. **(* indicates mean differ significantly from wild-type; P>0.001).**

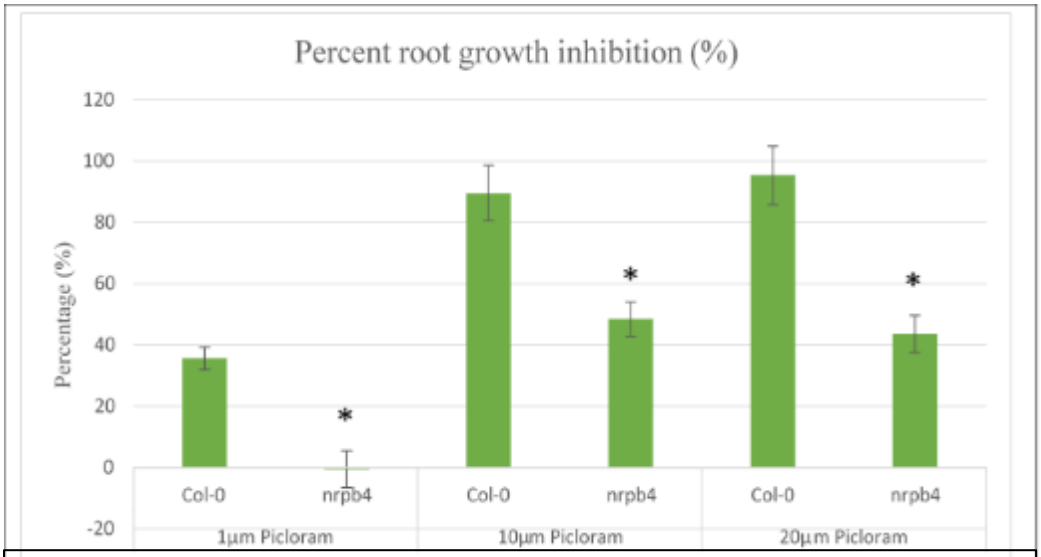

Figure 19. nrpb4 mutant showing resistance to auxin Picloram.
Col-0 and *nrpb4* mutant grown on ATS (1%). The four-day old seedlings were transferred on to Picloram (1µM; 10µM and 20µM) and incubated for two days. The percent root growth inhibition was calculated, and the data was analyzed using ANOVA. **(* indicates mean differ significantly from wild-type; P>0.001).**

Auxin-responsive gene expression is altered in *ibr5-1* and *nrpb4* mutants.

The auxin response genes *IAA7*, *IAA14*, *GH-3.3*, *GH-3.5*, *SAUR9* and *SAUR19* were selected to analyze in wild-type, *ibr5-1* and *nrpb4* mutants. It has been previously shown that the expression of these genes was highly inducible in response to auxin [44]. *Arabidopsis* seedlings were grown on ATS (1%) medium for four days and RNA was isolated from seedlings mock-treated or treated with 10µM 2,4-D for 1 hour. cDNA was generated using reverse transcription and used as a template for qRT- PCR to compare the relative expression and auxin-induced expression levels of the above-mentioned genes in *ibr5-1* and *nrpb4* mutant backgrounds [Figure 20- Figure 25]. The observed differences in the expression of auxin-responsive genes co-relates to the auxin insensitive phenotypes of *nrpb4* mutants.

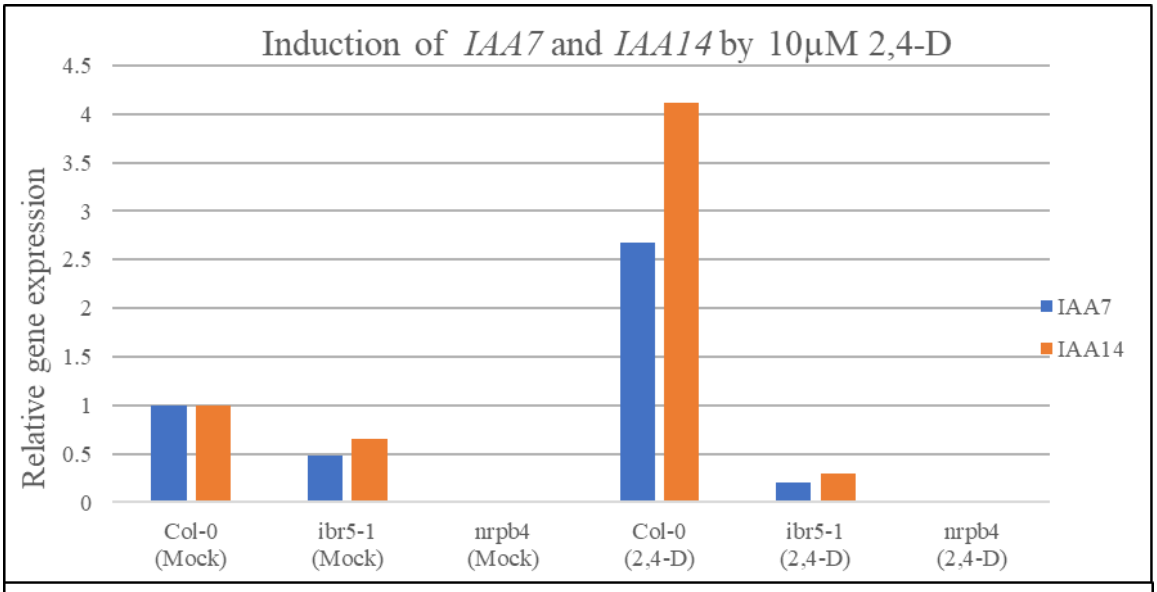

Figure 20. Induction of *IAA7* and *IAA14* genes in *ibr5-1* and *nrpb4* mutants. *Col-0*, *ibr5-1* and *nrpb4* mutants grown on ATS (1%). The four- day old seedlings were mock treated and treated with 10µM 2,4-D for 1 hour. The data shows the induction of auxin responsive genes.

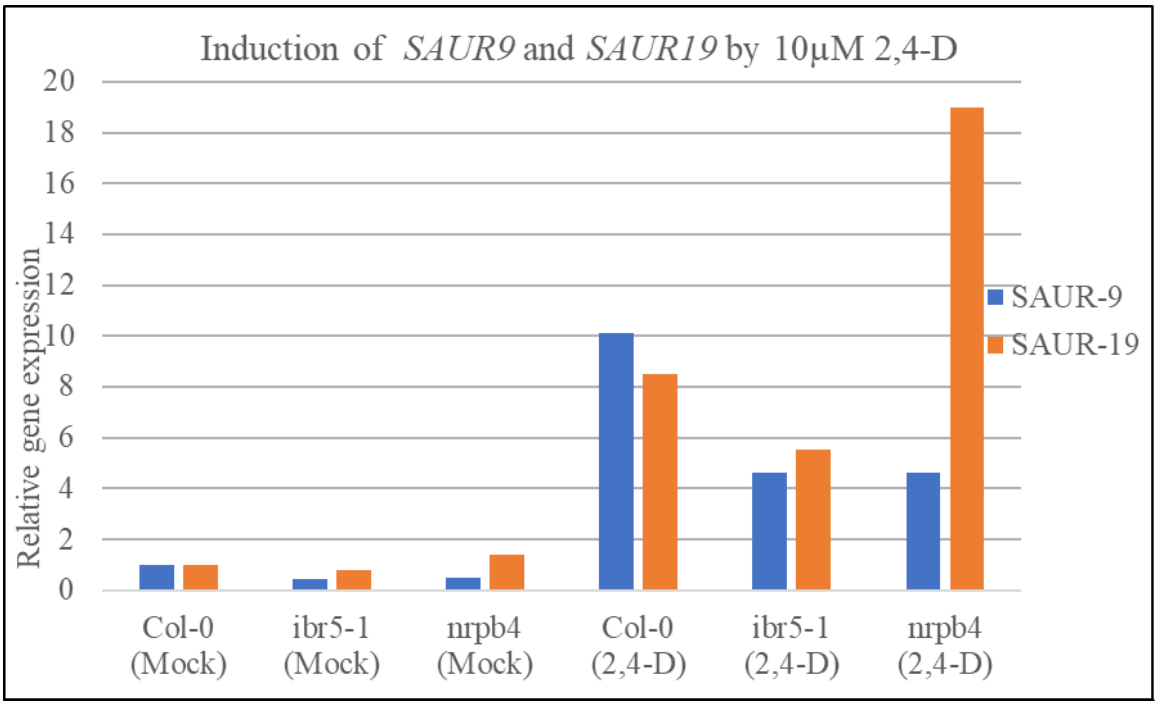

Figure 21. Induction of *SAUR9* and *SAUR19* genes in *ibr5-1* and *nrpb4* mutants. *Col-0*, *ibr5-1* and *nrpb4* mutants grown on ATS (1%). The four- day old seedlings were mock treated and treated with 10µM 2,4-D for 1 hour. The data shows the induction of auxin responsive genes.

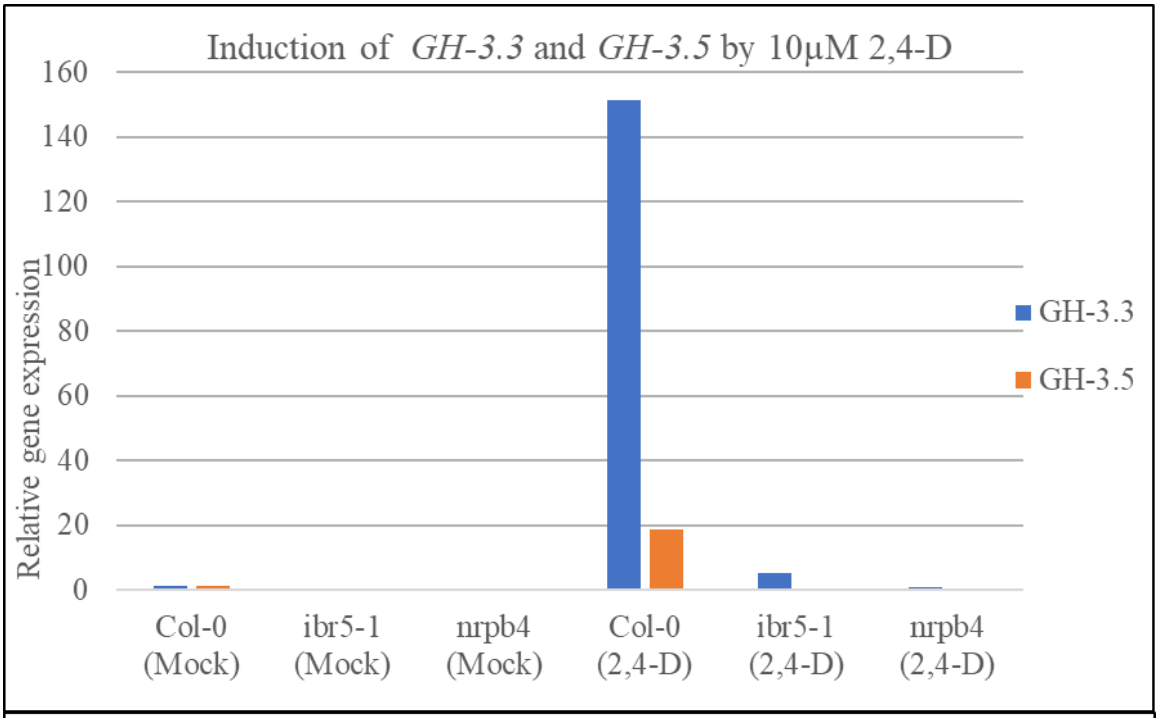

Figure 22. Induction of *GH-3.3* and *GH-3.5* genes in *ibr5-1* and *nrpb4* mutants. *Col-0*, *ibr5-1* and *nrpb4* mutants grown on ATS (1%). The four- day old seedlings were mock treated and treated with 10µM 2,4-D for 1 hour. The data shows the induction of auxin responsive genes.

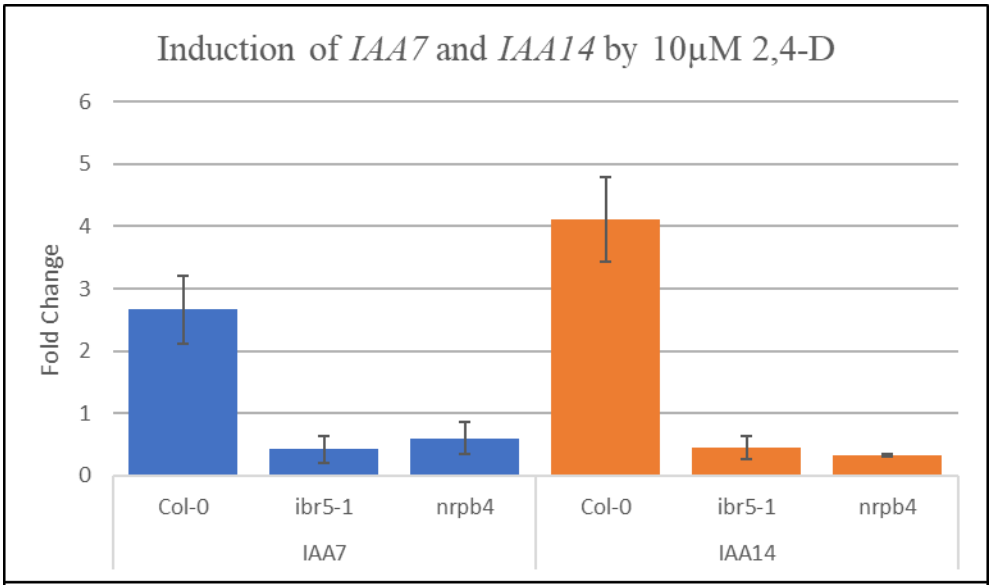

Figure 23. Induction of *IAA7* and *IAA14 by 10µM 2,4-D*. *Col-0*, *ibr5-1* and *nrpb4* mutants grown on ATS (1%). The four- day old seedlings were mock treated and treated with 10µM 2,4-D for 1 hour. The data shows the induction of auxin responsive genes. Error bars indicate Standard Error (SE).

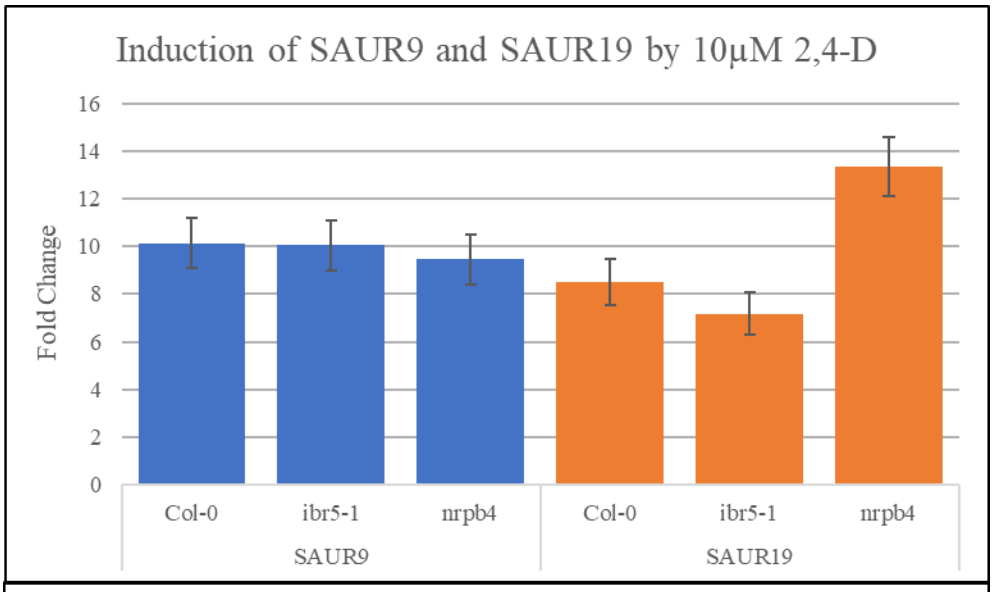

Figure 24. Induction of *SAUR9* and *SAUR19 by 10µM 2,4-D.* *Col-0*, *ibr5-1* and *nrpb4* mutants grown on ATS (1%). The four- day old seedlings were mock treated and treated with 10µM 2,4-D for 1 hour. The data shows the induction of auxin responsive genes. Error bars indicate Standard Error (SE).

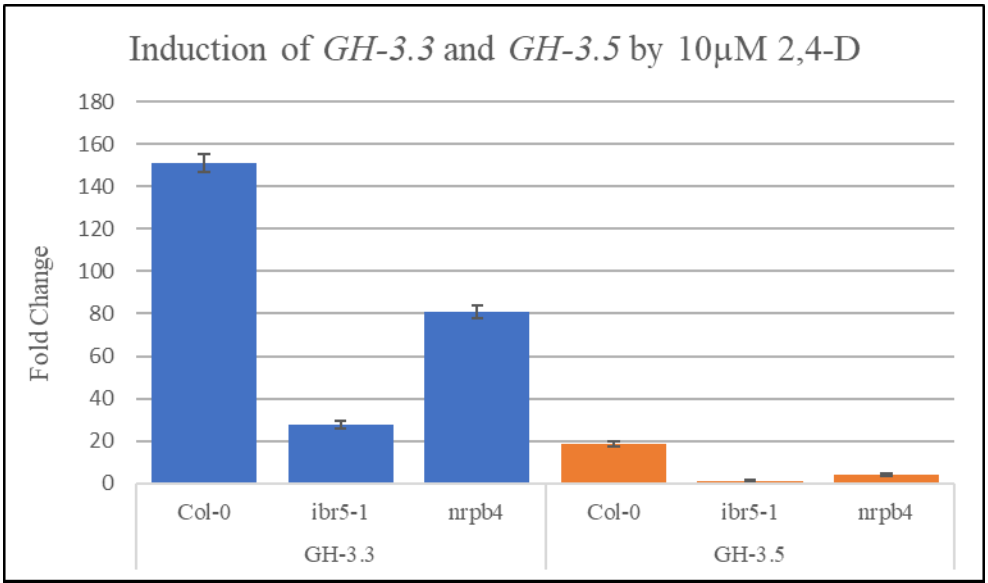

Figure 25. Induction of *GH-3.3* and *GH-3.5 by 10µM 2,4-D.* *Col-0*, *ibr5-1* and *nrpb4* mutants grown on ATS (1%). The four- day old seedlings were mock treated and treated with 10µM 2,4-D for 1 hour. The data shows the induction of auxin responsive genes. Error bars indicate Standard Error (SE).

IBR5 shows increased abundance at high temperature.

Since NRPB4 is shown to be involved in thermotolerance in yeast [24], and shows defective high-temperature response in Arabidopsis, the effect of high temperature on IBR5 was also studied.

Preliminary results with *ibr5* mutants showed increased hypocotyl length in comparison to wild type at 30^0C [*Cioffi, unpublished*]. Interestingly, when *IBR5:: IBR5-GUS* line was grown at 22^0C or 30^0C for four days in an incubator, increased IBR5-GUS expression was observed at 30^0C [Figure 26].

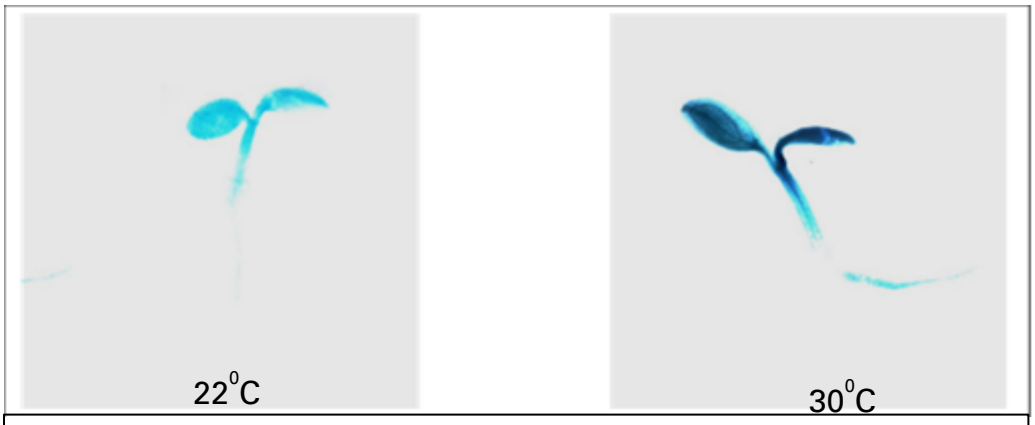

Figure 26. IBR5::IBR5-GUS expression at 22^0C and 30^0C.
Four days old seedlings showing the GUS expression at moderate and high temperature.

Interestingly, when tested the increased IBR5 abundance at high temperature using, *35S::IBR5-Myc* seedlings, IBR5-Myc abundance was higher in seedlings grown at 30^0C compared to the seedlings grown at 22^0C suggesting that high temperature mostly stabilizes IBR5, though other possibilities such as increased transcription or translation at high temperature cannot be excluded at this time [Figure 27].

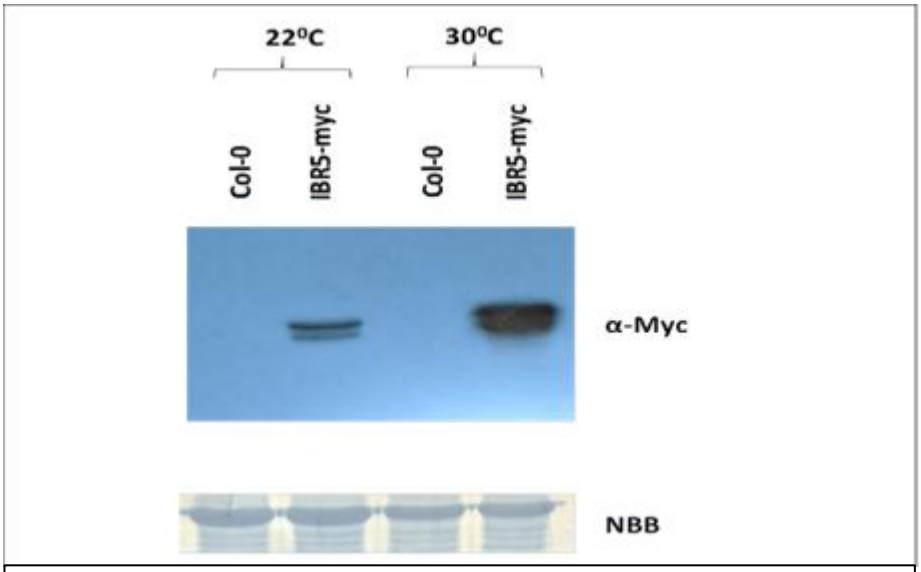

Figure 27. Western blot analysis of *35S::IBR5-myc*.
Four-day old seedlings show increase in the abundance of IBR5 protein level.

NRPB4 contains putative phosphorylation site within the protein sequence.

IBR5 has been shown to be a putative dual specificity phosphatase involved in dephosphorylating Ser/ Thr and Tyr amino acid residues [10]. For the proper functioning of RNA polymerase II in transcription, the C-terminal domain (CTD) of NRPB1 sub-unit must be phosphorylated and dephosphorylated for the activation and inactivation of the enzyme, respectively [49]. In yeast, it has also been shown that RPB4 interacts with

DSPs- Fcp1 and Ssu1 in order to help the DSPs association, accessibility and/or recruitment to the CTD [48]. Bioinformatic analysis using NetPhos2.0 software showed that NRPB4 has four putative phosphorylating sites at Ser18-P, Thr7-P, Tyr19-P, and Tyr23-P positions [Figure 28].

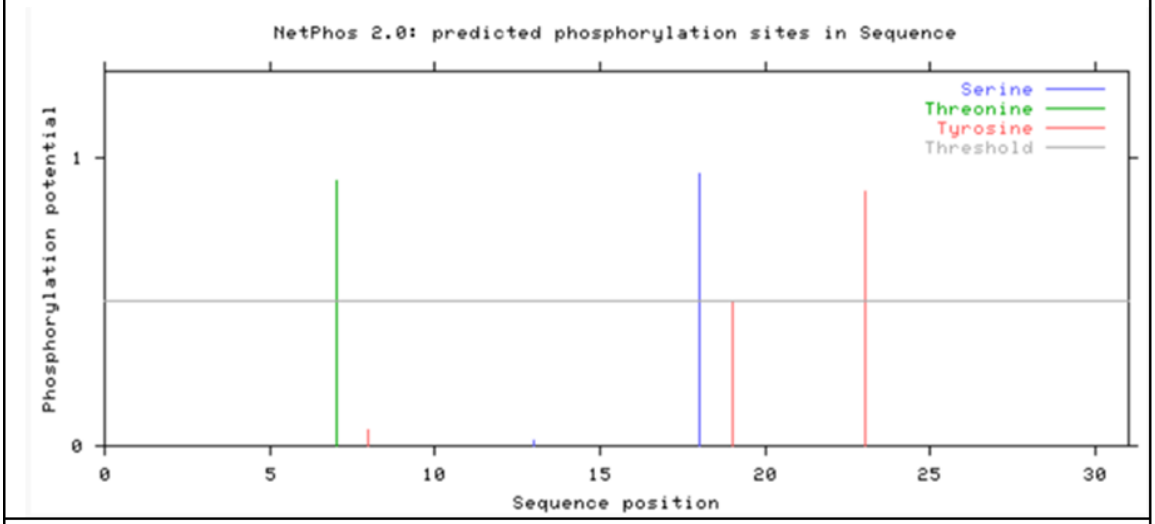

Figure 28. Potential phosphorylating sites as seen in NRPB4. Bioinformatics analysis revealed that NRPB4 had four potential phosphorylating sites at Thr7, Ser18, Tyr19, and Tyr23 positions.

IV. DISCUSSION

IBR5 physically interacts with NRPB4 *in-vitro.*

The preceding study showed an interaction between IBR5 and NRPB4 proteins in yeast two-hybrid screens [Kathare, unpublished]. If the interaction is true, it should help us understand how IBR5 and NRPB4 are involved in high-temperature response as both IBR5 [Cioffi, unpublished] and RPB4 [25 and Figure 4] are likely involved during heat stress responses. Interaction between these two proteins was detected *in vitro*, by pulling down IBR5-Myc (plant derived) with recombinant GST-NRPB4 [Figure 5]. However, the Co-IP assay show little of no *in-vivo* interaction. The negative result for the Co-IP and BiFC might be due to technical conditions not duly met for the assay to exhibit positive result, or certain physiological conditions that influence the interaction such as growth conditions of the plants or sub-cellular localization, and not necessarily the absence of interaction between these two proteins within the plants. Therefore, it may be crucial to try and use other *in-vivo* protein-protein interaction assays such as FRET-SE or Split-luciferase assays to confirm *in-vivo* protein-protein interaction as this interaction could be transient.

As previously mentioned, IBR5, a putative dual specificity phosphatase, has been shown to interact with and dephosphorylate MPK12 [12]. It has also been shown to act as a holdase and is involved in stabilizing CHS3 by associating with SGT1b and HSP90 [11]. In our lab, multiple IBR5 interacting proteins were identified such as CaM1, CaM3 [Jayaweera, unpublished], SCF complex component ASK1 [Jayaweera, unpublished], and several GTPases [Lopez, 2015 and Ghimre, 2015]. With all these above-mentioned IBR5 interacting proteins, it is fair to say that IBR5 may play a role in multiple cellular

processes. The IBR5-AtNRPB4 interaction is of interest as it might shed light on IBR5's function during heat stress in plants.

Catalytic domain and CBD of IBR5 are involved in IBR5-NRPB4 interaction.

In-vitro interaction assay with the deletion constructs of IBR5 provided valuable information about the regions with which NRPB4 interacts. Interaction of NRPB4 with D6 region of IBR5 suggests that calmodulin binding domain (CBD) and the catalytic domain that overlaps with CBD may be important for the interaction with NRPB4 [Figure 7].

N- and C- termini regions of NRPB4 are involved in IBR5-NRPB4 interaction.

In this study, it was observed that IBR5 interacted with both N- and C-termini of NRPB4 *in-vitro* [Figure 9b], suggesting that amino acid residues in both termini may be necessary for IBR5-NRPB4 interaction. The mid-region of RPB4 did not interact with IBR5 [Figure 9b]. In yeast, the results suggest that RPB4 has a conserved N- and C-termini and a non-conserved mid-region and RPB7 has been shown to interact with the conserved N- and C- termini and not the non-conserved mid-region of RPB4 [14].

IBR5-NRPB4 interaction is modulated by Ca^{2+}/CaM.

Previous work in our lab showed that IBR5 interacts with CaM in Ca^{2+} dependent manner indicating that IBR5 is a calmodulin binding protein (CaMBP) that contains a CBD. Interestingly, it was observed that the interaction between IBR5-NRPB4 increased upon addition of a Ca^{2+} ion chelator ethylene glycol-bis (β-aminoethyl ether) tetra-acetic acid [EGTA] [Figure 8]. Ca^{2+} ions act as an important component in signal transduction and plant development [38, 39 and 40]. CaMs are regulatory proteins that change their conformation when bound to Ca^{2+} ions. This conformational change allows them to

interact and thereby to modulate the functions of CaMBPs that include protein phosphatases, kinases and other metabolic enzymes [41 and 42]. Increased interaction between IBR5 and NRPB4 in the presence of EGTA, suggests that this interaction is modulated by Ca^{2+}/CaM.

***nrpb4* mutants show heat-related growth defective phenotype.**

The root growth analysis revealed that *nrpb4* mutants had significantly short stature including short roots at moderate (22^0C) as well as high (30^0C) temperatures [Figure 10 and Figure 11]. Previous work has shown that yeast RPB4 is mainly involved in mRNA synthesis. The deletion of yeast RPB4 decreases mRNA synthesis, and this defect is significantly enhanced at high temperature [32]. Arabidopsis *nrpb4* mutant also shows pleotropic growth defects at moderate temperature, but these defects are significantly more affected at high temperature as observed in primary root growth [Figure11a] and hypocotyl [Figure 11b]. In Arabidopsis, high temperature enhanced the hypocotyl elongation through increased auxin biosynthesis [43]. Since *nrpb4* mutants showed a significant defect in hypocotyl elongation at high temperature, it is possible that auxin responses are affected due to this mutation.

Auxin response is altered in *nrpb4*.

Since *nrpb4* mutants showed decreased hypocotyl elongation at high temperature, primary root growth response to exogenous auxin was tested using IAA, IBA, 2,4-D and Picloram. Interestingly, data show that the primary root growth of *nrpb4* is significantly insensitive to all exogenous auxins compared to wild-type [Figure 12 to Figure 19].

To analyze the observed auxin resistant phenotype, changes in relative gene expression of auxin-responsive genes- *IAA7*, *IAA14*, *GH-3.3*, *GH-3.5*, *SAUR9*, and

SAUR19, were quantified in *ibr5-1* and *nrpb4* mutants relative to wild-type. The expression of the above-mentioned genes was quantified using four-day-old seedlings that were mock treated or treated with 10µM 2,4-D, using qRT-PCR. The expression of all the genes was lower in *ibr5-1* than in wild-type, while the expression of *IAA7*, *IAA14*, *GH-3.3*, *GH-3.5*, and *SAUR9* was significantly lower in *nrpb4* mutants suggesting the correlation with the observed auxin- resistance phenotypes of *nrpb4* mutants. Interestingly, the expression of *SAUR19* was significantly higher in *nrpb4* mutants compared to wild-type. *SAUR19* helps in regulating cell expansion by regulating cellular auxin transport [45] [Figure 20 to Figure 25]. A Previous study in yeast reveals that under moderate conditions *Δrpb4* strains show defective transcription of many genes including a subset of genes involved in carbon and energy metabolism such as *GAL1*, *GAL10*, *HSE*, *PHO5*, and *INO1* [53]. However, the genes analyzed in Arabidopsis, for relative expression make-up a small representative subset of genes, which might not depict the effect of these mutations on auxin-responsive gene expression.

IBR5 expression is modulated by high temperature.

As previously described *Δrpb4* show defective growth phenotype at high temperature [Figure 5] and it has also been suggested that RPB4 is involved in thermotolerance in yeast [24]. Preliminary results of *ibr5* mutants showed increased hypocotyl elongation when treated with high temperature (30^0C) [*Cioffi, unpublished*].

Histochemical staining of four-day-old seedlings of *IBR5::IBR5-GUS* grown at 22^0C and 30^0C showed a significant increase in the levels of GUS at high temperature [Figure 26]. Furthermore, western analysis of *35S::IBR5-Myc* line grown at 22^0C and 30^0C for four days revealed an increase in abundance of IBR5 suggesting stabilization of

IBR5 at high temperature [Figure 27]. A previous study in Arabidopsis suggest an enhanced functioning of *AtPP5*, a multifunctional protein acting as holdase chaperone, foldase chaperone and protein phosphatase; in holdase chaperone activity at high temperature [54]. Similarly, in IBR5, it is likely to suggest that it might be necessary for stabilization of IBR5 at high temperature to properly function as a chaperone. But, the results showing the stabilization of IBR5 at a high temperature cannot be proven at this point as other possibilities such as increased transcription or translation cannot be excluded.

Conclusions and future directions

Though several proteins were found to be interacting with IBR5, it is still unclear how the role of IBR5 can be implicated in auxin signaling. Based on the results conferred in this study, it can be deduced that IBR5, a putative dual specificity phosphatase, physically interacts with NRPB4 *in-vitro* [Figure 5]. Furthermore, it was also confirmed that specific domains of IBR5 are involved in the interaction with NRPB4 [Figure 7]. These results suggest that the catalytic domain and the calmodulin-binding domain (CBD) of IBR5 along with certain amino acid sequences surrounding the CBD are important for this interaction with NRPB4. Subsequently, it was also observed that C- and N- termini of NRPB4 are involved in the interaction with IBR5, suggesting the presence of amino acid sequence in this region promoting the interaction with IBR5. Additionally, it was also observed that IBR5-NRPB4 interaction increased *in-vitro* upon chelating Ca^{2+} ions whenever EGTA was added to the protein extracts, suggesting the interaction between these two proteins is modulated by Ca^{2+}/CaM [Figure 8].

The homozygous T-DNA insertional mutant of *nrpb4* procured from ABRC,

showed stunted growth at moderate temperature (22^0C) and hardly produced any seeds, suggesting a pleotropic developmental defect [Figure 10 and Figure 11]. This may suggest defects in total mRNA synthesis as observed previously in yeast [33]. Additionally, the results also showed that *nrpb4* mutants had defective hypocotyl elongation at high temperature (30^0C) [Figure11b], hinting its role in the auxin mediated response. The role of NRPB4 in auxin signaling pathway was further strengthened by the result, *nrpb4* mutants showing an auxin resistance root-growth phenotype in response to exogenous auxin [Figure12 to Figure19]. This result was further supported by decreased transcript level of auxin responsive genes in *nrpb4* mutant compared to wild-type [Figure 20 to Figure 25]. However, further work such as degradation of *AUX/IAA* proteins in the *nrpb4* mutants is needed to confirm the auxin specific effect, as the effect we are seeing could be due to the manifestation of general growth defects.

The possible role of IBR5-NRPB4 interaction can be justified using the hypothetical model [Figure 29]. In yeast, it has been shown that RPB4 and RPB7 acts as a heterodimer and are involved in mediating transcription initiation, elongation, polyadenylation [46] and dephosphorylation of C-terminal domain (CTD) of RPB1 [47 and 48]. Fcp1, a phosphatase in yeast is involved in dephosphorylation of Ser2-P, while other two phosphatases, Rtr1 and Ssu1, associate with each other and dephosphorylates Ser5-P during transcriptional elongation and termination respectively [49]. Using EMBOSS Needle software from EMBL-EBI, the amino acid sequence of Fcp1 was aligned with IBR5, it showed 16.5% (i.e., 135 out of 257 amino acids in IBR5) sequence similarity. Though there is no great similarity between Fcp1 and IBR5, in plants, IBR5 might be involved in dephosphorylation of CTD of NRPB1 in Arabidopsis. IBR5-AtNRPB4

interaction might play an important role in dephosphorylating NRPB1. Furthermore, bioinformatic analysis using NetPhos2.0 software showed that NRPB4 has some putative phosphorylating sites at Ser18-P, Thr7-P, Tyr19-P and Tyr23-P positions [Figure 28] and IBR5 being a putative DSP, there is a possibility that IBR5 dephosphorylates NRPB4 and helps in the dissociation of NRPB4 from RNA polymerase II holoenzyme to deactivate

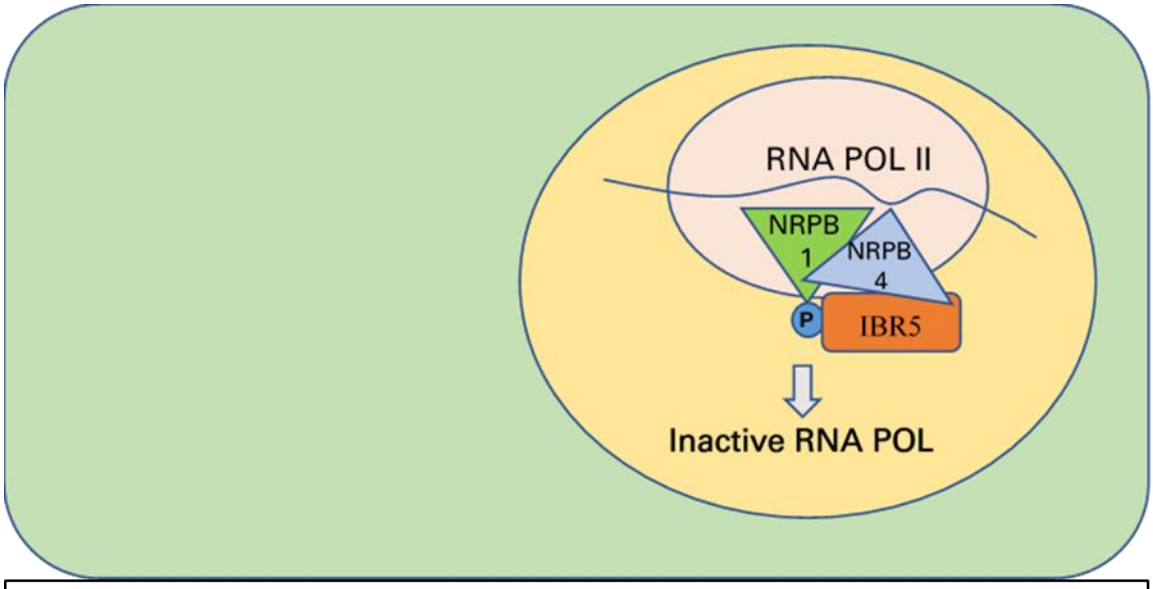

Figure 29. Hypothetical model showing the possible function of IBR5-NRPB4 interaction.
IBR5-NRPB4 interaction might help in dephosphorylating CTD of NRPB1 in order to inactivate RNA POL II to control the transcription.

the enzyme in order to terminate mRNA synthesis.

Moreover, during heat stress in eukaryotes, HSP90 is involved in the prevention of aggregation of unfolded proteins [50]. In yeast, it has been previously shown that RPB4 is involved in thermotolerance [24]. Additionally, IBR5 has shown to interact with CHS3 and forms a complex with SGT1b and HSP90 to protect CHS3 [11] and in another study, it has been shown that HSP90 interacts with PB1 and PB2 sub-units of viral RNA Polymerase and involved in the nuclear transport and assembly of the viral RNA Pol sub-units [52]. The result from this study also suggests the elevation in the abundance of

IBR5 protein level at high temperature [Figure 27 and Figure 28]. From all the above-mentioned observations, it can be suggested that HSP90, IBR5 and NRPB4 may function as a complex in recovering the plants from heat stress. If this hypothesis holds true, it can also be proved that NRPB4 has independent functions in Arabidopsis apart from it being an integral part of RNA Pol II.

REFERENCES

1. Teale, W., Paponov, I. and Palme, K. (2006). Auxin in action: signaling, transport and the control of plant growth and development. *Nature Reviews Molecular Cell Biology*, 7(11), pp.847-859.
2. Ulmasov, T., Hagen, G. and Guilfoyle, T. (1999). Activation and repression of transcription by auxin-response factors. *Proceedings of the National Academy of Sciences*, 96(10), pp.5844-5849.
3. Tiwari, S., Wang, X., Hagen, G. and Guilfoyle, T. (2001). AUX/IAA Proteins Are Active Repressors, and Their Stability and Activity Are Modulated by Auxin. *The Plant Cell*, 13(12), p.2809.
4. Gray, W., Kepinski, S., Rouse, D., Leyser, O. and Estelle, M. (2001). Auxin regulates SCFTIR1-dependent degradation of AUX/IAA proteins. *Nature*, 414(6861), pp.271-276.
5. Dharmasiri, S., Jayaweera, T. and Dharmasiri, N. (2013). Plant Hormone Signalling: Current Perspectives on Perception and Mechanisms of Action. *Ceylon Journal of Science (Biological Sciences)*, 42(1), p.1.
6. Choi, C., Gray, W., Mooney, S. and Hellmann, H. (2014). Composition, Roles, and Regulation of Cullin-Based Ubiquitin E3 Ligases. *The Arabidopsis Book*, 12, p.e0175.
7. Yu, H., Zhang, Y., Moss, B., Bargmann, B., Wang, R., Prigge, M., Nemhauser, J. and Estelle, M. (2015). Untethering the TIR1 auxin receptor from the SCF complex increases its stability and inhibits auxin response. *Nature Plants*, 1(3).

8. Dharmasiri, N., Dharmasiri, S. and Estelle, M. (2005). The F-box protein TIR1 is an auxin receptor. *Nature*, 435(7041), pp.441-445.
9. Strader, L., Monroe-Augustus, M. and Bartel, B. (2008). The IBR5 phosphatase promotes Arabidopsis auxin responses through a novel mechanism distinct from TIR1-mediated repressor degradation. *BMC Plant Biology*, 8(1), p.41.
10. Jayaweera, T., Siriwardana, C., Dharmasiri, S., Quint, M., Gray, W. and Dharmasiri, N. (2014). Alternative Splicing of Arabidopsis IBR5 Pre-mRNA Generates Two IBR5 Isoforms with Distinct and Overlapping Functions. *PLoS ONE*, 9(8), p.e102301.
11. Liu, J., Yang, H., Bao, F., Ao, K., Zhang, X., Zhang, Y. and Yang, S. (2015). IBR5 Modulates Temperature-Dependent, R Protein CHS3-Mediated Defense Responses in Arabidopsis. *PLOS Genetics*, 11(10), p.e1005584.
12. Lee, J., Wang, S., Sritubtim, S., Chen, J. and Ellis, B. (2009). Arabidopsis mitogen-activated protein kinase MPK12 interacts with the MAPK phosphatase IBR5 and regulates auxin signaling. *The Plant Journal*, 57(6), pp.975-985.

13. Dreze, M., Carvunis, A., Charloteaux, B., Galli, M., Pevzner, S., Tasan, M., Ahn, Y., Balumuri, P., Barabasi, A., Bautista, V., Braun, P., Byrdsong, D., Chen, H., Chesnut, J., Cusick, M., Dangl, J., de los Reyes, C., Dricot, A., Duarte, M., Ecker, J., Fan, C., Gai, L., Gebreab, F., Ghoshal, G., Gilles, P., Gutierrez, B., Hao, T., Hill, D., Kim, C., Kim, R., Lurin, C., MacWilliams, A., Matrubutham, U., Milenkovic, T., Mirchandani, J., Monachello, D., Moore, J., Mukhtar, M., Olivares, E., Patnaik, S., Poulin, M., Przulj, N., Quan, R., Rabello, S., Ramaswamy, G., Reichert, P., Rietman, E., Rolland, T., Romero, V., Roth, F., Santhanam, B., Schmitz, R., Shinn, P., Spooner, W., Stein, J., Swamilingiah, G., Tam, S., Vandenhaute, J., Vidal, M., Waaijers, S., Ware, D., Weiner, E., Wu, S. and Yazaki, J. (2011). Evidence for Network Evolution in an Arabidopsis Interactome Map. *Science*, 333(6042), pp.601-607.
14. Sampath, V., Rekha, N., Srinivasan, N. and Sadhale, P. (2003). The Conserved and Non-conserved Regions of Rpb4 Are Involved in Multiple Phenotypes in Saccharomyces cerevisiae. *Journal of Biological Chemistry*, 278(51), pp.51566-51576.
15. Kipreos, E. T. and Pagano, M. (2000). The F-box protein family. *Genome Biology 1(5)*, 3002.1-3002.7.
16. Meka, H., Werner, F., Cordell, S., Onesti, S., and Brick, P. (2005). Crystal structure and RNA binding of the Rpb4/Rpb7 subunits of human RNA polymerase II. *Nucleic Acids Research,33*(19), 6435-6444.
17. Monroe-Augustus, M. (2003). IBR5, a Dual-Specificity Phosphatase-Like Protein Modulating Auxin and Abscisic Acid Responsiveness in Arabidopsis. *THE PLANT CELL ONLINE*, 15(12), pp.2979-2991.

18. Shimizu-Mitao, Y., and Kakimoto, T. (2014). Auxin Sensitivities of All Arabidopsis Aux/IAAs for Degradation in the Presence of Every TIR1/AFB. *Plant and Cell Physiology,55*(8), 1450-1459.
19. Rogg, L., Lasswell, J., and Bartel, B. (2001). A Gain-of-Function Mutation in IAA28 Suppresses Lateral Root Development. *The Plant Cell,13*, 465-480.
20. Ulmasov, T., Murfett, J., Hagen, G., & Guilfoyle, T. J. (1997). Aux/IAA Proteins Repress Expression of Reporter Genes Containing Natural and Highly Active Synthetic Auxin Response Elements. *The Plant Cell,9*(11), 1963.
21. Hagecalvon, G., & Guilfoyle, T. (2002). Auxin-responsive gene expression: Genes, promoters and regulatory factors. *Auxin Molecular Biology,*373-385.
22. Kornberg, R. D. (1999). Eukaryotic transcriptional control. *Trends in Cell Biology,9*(12).
23. Sims, R. J., Mandal, S. S., & Reinberg, D. (2004). Recent highlights of RNA-polymerase-II-mediated transcription. *Current Opinion in Cell Biology,16*(3), 263-271.
24. Larkin, R. M., & Guilfoyle, T. J. (1998). Two Small Subunits in Arabidopsis RNA Polymerase II Are Related to Yeast RPB4 and RPB7 and Interact with One Another. *Journal of Biological Chemistry,273*(10), 5631-5637.
25. Rosenheck, S., & Choder, M. (1998). Rpb4, a Subunit of RNA Polymerase II, Enables the Enzyme To Transcribe at Temperature Extremes In Vitro. *J. Bacteriology,180*(23), 6187-6192.

26. Sampath, V., Balakrishnan, B., Verma-Gaur, J., Onesti, S., & Sadhale, P. P. (2007). Unstructured N Terminus of the RNA Polymerase II Subunit Rpb4 Contributes to the Interaction of Rpb4·Rpb7 Subcomplex with the Core RNA Polymerase II of Saccharomyces cerevisiae. *Journal of Biological Chemistry,283*(7), 3923-3931.
27. Gray, W. M., Ostin, A., Sandberg, G., Romano, C. P., & Estelle, M. (1998). High temperature promotes auxin-mediated hypocotyl elongation in Arabidopsis. *Proceedings of the National Academy of Sciences,95*(12), 7197-7202.
28. Dharmasiri, N., Dharmasiri, S., Weijers, D., Lechner, E., Yamada, M., Hobbie, L., Ehrismann, J., Jürgens, G.,Estelle, M. (2005). Plant Development Is Regulated by a Family of Auxin Receptor F Box Proteins. *Developmental Cell,9*(1), 109-119.
29. Clough, S.J., and Bent, A.F. (1998). Floral dip: a simplified method for Agrobacterium mediated transformation of Arabidopsis thaliana. Plant J 16, 735-743.
30. Bradford, M.M. (1976). A rapid and sensitive method for the quantitation of microgram quantities of protein utilizing the principle of protein-dye binding. Anal Biochem 72, 248-254.
31. Schweiger, R., and Schwenkert, S. (2014). Protein-protein Interactions Visualized by Bimolecular Fluorescence Complementation in Tobacco Protoplasts and Leaves. *Journal of Visualized Experiments,* (85). doi:10.3791/51327.
32. Schulz, D., Pirkl, N., Lehmann, E., and Cramer, P. (2014). Rpb4 Subunit Functions Mainly in mRNA Synthesis by RNA Polymerase II. *Journal of Biological Chemistry,289*(25), 17446-17452.

33. Choder, M., and Young, R. A. (1993). A portion of RNA polymerase II molecules has a component essential for stress responses and stress survival. *Molecular and Cellular Biology,13*(11), 6984-6991.

34. Livak, K. J., and Schmittgen, T. D. (2001). Analysis of Relative Gene Expression Data Using Real-Time Quantitative PCR and the 2−ΔΔCT Method. *Methods,25*(4), 402-408.

35. Gray, W. M., del Pozo, J. C., Walker, L., Hobbie, L., Risseeuw, E., Banks, T., Crosby, W. L., Yang, M., Ma. H., and Estelle, M. (1999) Identification of an SCF ubiquitin ligase complex required for auxin response in Arabidopsis thaliana. Genes Dev 13(13), 1678-1691.

36. Armache, K., Kettenberger, H., and Cramer, P. (2003). Architecture of initiation-competent 12-subunit RNA polymerase II. *Proceedings of the National Academy of Sciences,100*(12), 6964-6968.

37. Ream, T. S., Haag, J. R., Wierzbicki, A. T., Nicora, C. D., Norbeck, A. D., Zhu, J., Hagen, G., Guilfoyle, T., Pasa-Tolic, L.,and Pikaard, C. S. (2009). Subunit Compositions of the RN`A-Silencing Enzymes Pol IV and Pol V Reveal Their Origins as Specialized Forms of RNA Polymerase II. *Molecular Cell,33*(2), 192-203.

38. Kudla, J., Batistic, O., and Hashimoto, K. (2010). Calcium signals: the lead currency of plant information processing. Plant Cell 22(3), 541-563.

39. Hepler, P. K., and Wayne, R. O. (1985). Calcium and plant development. Annu. Rev. Plant Physiol. 36, 397-439.

40. Bush, D. S. (1995). Calcium regulation in plant cells and its role in signaling. Annu. Rev. Plant Physiol. 46, 95-122.

41. Perochon, A., Aldon, D., Galaud, J. P., and Ranty, B. (2011). Calmodulin and calmodulin like proteins in plant calcium signaling. Biochimie. 93(12), 2048-2053.

42. Bouché, N., Yellin, A., Snedden, W. A., and Fromm, H. (2005). Plant-specific calmodulin-binding proteins. Annu. Rev. Plant Physiol. 56, 435-466.

43. Franklin, K. A., Lee, S. H., Patel, D., Kumar, S. V., Spartz, A. K., Gu, C., Ye, S., Yu, P., Breen, G., Cohen, J. D., Wigge, P. A., and Gray, W. M. (2011) PHYTOCHROME INTERACTING FACTOR 4 (PIF4) regulates auxin biosynthesis at high temperature. Proc Natl Acad Sci 108(50), 20231-20235.

44. Goda, H., Sasaki, E., Akiyama, K., Maruyama-Nakashita, A., Nakabayashi, K., Li, W., Ogawa, M., Yamauchi, Y., Preston, J., Aoki, K., Kiba, T., Takatsuto, S., Fujioka, S., Asami, T., Nakano, T., Kato, H., Mizuno, T., Sakakibara, H., Yamaquchi, S., Nambara, E., Kamiya, Y., Takahashi, H., Hirai, M. Y., Sakurai, T., Shinozaki, K., Saito, K., Yoshida, S., and Shimada, Y. (2008). The AtGenExpress hormone and chemical treatment data set: experimental design, data evaluation, model data analysis and data access. Plant J 55(3), 526-542.

45. Spartz, A. K., Lee, S. H., Wenger, J. P., Gonzalez, N., Itoh, H., Inzé, D., Peer, W., Murphy, A., and Gray, W. M. (2012). The SAUR19 subfamily of SMALL AUXIN UP RNA genes promote cell expansion. *The Plant Journal,70*(6), 978-990.

46. Runner, V. M., Podolny, V., and Buratowski, S. (2008). The Rpb4 Subunit of RNA Polymerase II Contributes to Cotranscriptional Recruitment of 3 Processing Factors. *Molecular and Cellular Biology,28*(6), 1883-1891.

47. Kamenski, T., Heilmeier, S., Meinhart, A., and Cramer, P. (2004). Structure and Mechanism of RNA Polymerase II CTD Phosphatases. *Molecular Cell*,*15*(3), 399-407.

48. Allepuz-Fuster, P., Martínez-Fernández, V., Garrido-Godino, A. I., Alonso-Aguado, S., Hanes, S. D., Navarro, F., and Calvo, O. (2014). Rpb4/7 facilitates RNA polymerase II CTD dephosphorylation. *Nucleic Acids Research*,*42*(22), 13674-13688.

49. Zhang, D. W., Rodríguez-Molina, J. B., Tietjen, J. R., Nemec, C. M., and Ansari, A. Z. (2012). Emerging Views on the CTD Code. *Genetics Research International*,*2012*, 1-19.

50. Richter, K., Haslbeck, M., and Buchner, J. (2010). The Heat Shock Response: Life on the Verge of Death. *Molecular Cell*,*40*(2), 253-266.

51. Larkindale, J., Hall, J., Knight, M., & Vierling, E. (2005). Heat Stress Phenotypes of Arabidopsis Mutants Implicate Multiple Signaling Pathways in the Acquisition of Thermotolerance. *Plant Physiology*,*138*(2), 882-897.

52. Naito, T., Momose, F., Kawaguchi, A., & Nagata, K. (2006). Involvement of Hsp90 in Assembly and Nuclear Import of Influenza Virus RNA Polymerase Subunits. *Journal of Virology*,*81*(3), 1339-1349.

53. Pillai, B., Sampath, V., Sharma, N., & Sadhale, P. (2001). Rpb4, a Non-essential Subunit of Core RNA Polymerase II ofSaccharomyces cerevisiaeIs Important for Activated Transcription of a Subset of Genes. *Journal of Biological Chemistry*,*276*(33), 30641-30647.

54. Park, J. H., Lee, S. Y., Kim, W. Y., Jung, Y. J., Chae, H. B., Jung, H. S., Kang, H. C., Shin, R. M., Kim, Y. S., Su'Udi, M., Yun, J. D., Lee, O. K., Kim, H. M., and Lee, S. Y. (2011). Heat-induced chaperone activity of serine/threonine protein phosphatase 5 enhances thermotolerance in Arabidopsis thaliana. *New Phytologist*,*191*(3), 692-705.

55. Sambrook, J., Fritsch, E. F., & Maniatis, T. (2012). *Molecular cloning: A laboratory manual*. Cold Spring Harbor: Cold Spring Harbor Laboratory Press.